THE EFFECT OF LONG-TERM SUCROSE CONSUMPTION ON OLFACTORY NEUROGENESIS AND NEUROINFLAMMATION

Catherine Keys

BBiomedSc

Submitted in fulfilment of the requirements for the degree of

Master of Philosophy

School of Biomedical Sciences

Faculty of Health

Queensland University of Technology

2023

Keywords

5-Ethynyl-2'-deoxyuridine (EdU), Adolescent, Astrocyte, Calbindin, Calretinin, Feeding pathway, Granule cells, Juxtaglomerular cells, Interneuron, Microglia, Neural Stem Cells, Neuroblasts, Neurogenesis, Obesity, Olfactory Bulb, Rostral Migratory Stream, Subventricular zone, Sucrose Consumption, Tyrosine Hydroxylase.

Abstract

The association between obesity and sucrose consumption has been well established. It has been found that sucrose consumption incurs many neurological and cognitive deficits. It has been previously reported that sucrose consumption reduced hippocampal neurogenesis and changed glial cells behaviour, however its effects on other neurogenic areas such as the subventricular (SVZ) remain unclear. Therefore, we studied the effects of long-term sucrose on a well-established drinking mouse model with *ad libitum* access to a 25% sucrose drink for 13 weeks. The results showed that there were no changes to SVZ neurogenesis. However, there was a reduction of neuroblasts in the vertical arm of the rostral migratory stream (RMS) with no change in the elbow of the RMS. At the level of the olfactory bulb (OB), sucrose consumption was found to cause an increase in the population of calbindin juxtaglomerular cells, however there were no changes to the populations of calretinin, tyrosine hydroxylase juxtaglomerular cells, and granule cell populations. The data regarding glial cell behaviours did not show any significant changes to the microglia of the SVZ, RMS or OB however, sucrose consumption affected astrocyte behaviour in these regions. All together, these results contribute to the growing body of research surrounding the effect of diet on the neurogenic regions of the brain which leads to cognitive deficits.

Table of Contents

List of Figures

List of Tables

List of Abbreviations

AL: *Ad libitum*

BDNF: Brain-derived neurotrophic factor

CB: Calbindin

CNS: Central nervous system

CR: Calretinin

DCX: Doublecortin

EdU: 5-Ethynyl-2'-deoxyuridine

EPL: External Plexiform layer

ET: External tufted

GABA: γ-aminobutyric acid

GFAP: Glial fibrillary acidic protein

GL: Glomerular layer

GrL: Granular layer

IPL: Internal plexiform layer

MCL: Mitral cell layer

OB: Olfactory bulb

ONL: Olfactory nerve layer

PACE: Pharmacy Australia Centre of Excellence

PG: Periglomerular

RMS: Rostral migratory stream

sSA: Superficial short axon

SVZ: Subventricular Zone

TH: Tyrosine hydroxylase

TMEM119: Transmembrane protein 119

Acknowledgements

I would like to thank my primary supervisor Dr. Fatemeh Chehrehasa for providing the opportunity to complete this master's project. I would also like to thank her for all the support she provided me along the way. I would like to thank other supervisors Professor Selena Bartlett and D. Arnauld Belmer for their all the training, scientific expertise and guidance. I would like to acknowledge the School of Biomedical Science, the Faculty of Health and Queensland University of Technology for the opportunity to complete this research. This research was supported by QUT Scholarship funding.

I am thankful for the training I received from Rachel Smith and Lisa Foster at the University of Queensland's Biological Resources facility at the Pharmacy Australia Centre for Excellence. I also want to thank Dr. Cameron Flegg for all the training and assistance I received for microscopy imaging.

I would like to thank my friends and family who have been with me throughout this process. I am forever grateful for your continual support and encouragement. Above all I would like to thank God for all He has done for me.

Chapter 1: Introduction

1.1 Background

Obesity is highly prevalent in modern society (GBD 2015 Obesity Collaborators et al., 2017; OECD, 2019). With almost 60% of adults being overweight, of which 25% are classified as obese (OECD, 2019). It causes a number of health and financial burdens to the society (Apovian, 2016; PwC Australia, 2015) and individuals with obesity also endure a lower quality of life (Y.-K. Wu & Berry, 2018). The association between sugar consumption and obesity has received a lot of scrutiny, as it is known to drive weight gain and predict body mass index (Lin et al., 2018; Luger et al., 2017; Malik et al., 2013). Australian adolescents and children consume copious amounts of ultra processed, high-sugar foods, as it makes up for more than 50% of energy intake, far surpassing recommended 10% cutoff of energy consumption via free sugars (Machado et al., 2020). With the grave toll of obesity, and the excessive intake of sugar in modern diets, it is important to research the impact of this obesogenic diet on the brain.

The effects of sugar consumption on memory has been reported previously (Beecher, Alvarez Cooper, et al., 2021; Beilharz et al., 2014, 2016). Our lab recently found that long-term sucrose consumption causes deficits in spatial and episodic memory due to reductions in hippocampal (memory part of the brain) neurogenesis (Beecher, Alvarez Cooper, et al., 2021). The overconsumption of sugar-sweetened beverages have been shown to affect sleep quality and motor coordination, while also producing attention deficit hyperactivity disorder (ADHD) in children (Anjum et al., 2018). While these pathologies are more commonly known, the effect of sugar consumption on neurogenic areas of the forebrain remains obscure.

Neurogenesis is the process which involves the production of new neurons. There are only a few areas in the brain which undergo neurogenesis postnatally: the dentate gyrus of the hippocampus and the subventricular zone (SVZ) in rodents and humans (Abdissa et al., 2020; Lalli, 2014; Leiter et al., 2022). However, the topic of human neurogenesis remains highly controversial (Gage, 2019; Kempermann et al., 2018). It seems, SVZ neurogenesis declines in childhood (Coletti et al., 2018; Paredes et al., 2016; Wang et al., 2011). However, early-post-natal SVZ neurogenesis in humans has been proposed to have a necessary role in synaptic plasticity (Sanai et al., 2011). Therefore, this region remains a viable research avenue for assessing the effect of sugar consumption on forebrain adult neurogenesis.

The SVZ undergoes neurogenesis to send the newborn neurons, or neuroblasts, to the olfactory bulb. Once they have arrived at the olfactory bulb the neuroblasts then differentiate into olfactory interneurons, a cell type which aims to regulate the surrounding circuitry (Burton, 2017; Matsuno et al., 2017; Najac et al., 2015; Schoppa & Urban, 2003). Many lifestyle and dietary factors including glucose intake, vitamin C intake and physical activity have been found to affect SVZ neurogenesis (Jara et al., 2022; Lang et al., 2009; Nicolis di Robilant et al., 2019). However, the effect of long-term sucrose consumption on SVZ neurogenesis remains understudied. Additionally, obesogenic diets are known to cause neuroinflammation in the hypothalamus, the appetite hub of the brain (Gao et al., 2017; Horvath et al., 2010; Lainez et al., 2018). It has also been found that overactivation of glial cells in the hypothalamus causes an increases in appetite (Valdearcos et al., 2017). Given that the olfactory system does have an important role in appetite regulation (Palouzier-Paulignan et al., 2012), there is a need to study the glial cell behaviour of the olfactory system in response to sucrose consumption.

1.2 Hypothesis and Aims

The project aims to investigate the effect of long-term sucrose consumption on SVZ neurogenesis and the olfactory bulb which receive neurons from this region throughout life. Quantifying SVZ neurogenic cellular populations, and olfactory neuron populations along with assessing glial cell behaviour will be required to determine the effects of sucrose consumption on the olfactory system. It is hypothesised that sucrose consumption will cause deficits in SVZ neurogenesis, which will correlate with reduced olfactory interneuron populations. These reductions are expected alongside a more neuroinflammatory glial cell profile in the areas of the SVZ, rostral migratory stream and olfactory bulb. These hypotheses will be tested with the following aims:

Aim 1: To determine the effect of long-term sucrose consumption on SVZ neurogenesis and olfactory interneuron populations.

Aim 2: To determine the effect of long-term sucrose consumption on astrocyte and microglial behaviour (population and cell volume) of the SVZ, rostral migratory stream and olfactory bulb.

Chapter 2: Literature Review

2.1 Obesity

Obesity is a disease process characterized by an excessive accumulation of body fat which may result in health complications (Bray et al., 2017). In 2018, the Australian Bureau of Statistics found that 67% of Australian adults were overweight or obese (Australian Bureau of Statistics, 2018). In addition, the cumulative economic cost of obesity in Australia is estimated to reach $87.7 billion by 2025 (PwC Australia, 2015). Obese individuals are also at a higher risk of developing other comorbidities such as type 2 diabetes mellitus, coronary artery disease, stroke and some types of cancer (Apovian, 2016). The mental health of individuals with obesity is also likely to suffer, as there is a positive correlation between obesity and mental health conditions such as anxiety and depression (Gariepy et al., 2010; Luppino et al., 2010). In 2016, high body mass was recognized to have an immense contribution for total disease burden as it was ranked second only to tobacco consumption (Australian Institute of Health and Welfare, 2016). While long-term sugar consumption cannot be attributed as the sole cause of obesity (Bortolin et al., 2018; J. Li et al., 2020), it is still considered as a contributing dietary factor to the disease (de Oliveira Neves et al., 2020). Further, excessive sugar consumption has been suggested to lead to sugar addiction (Avena et al., 2008), which is an important factor in obesity as it drives the individual to maintain an excessive consumption of food or increase their caloric intake (Gaysinskaya et al., 2011), resulting in obesity. There is a growing collection of literature supporting the correlation between high caloric diets and declined cognitive function, including deficits in attentional bias and episodic memory (Beecher, Alvarez Cooper, et al., 2021; Gunstad et al., 2020). Given the grave toll of obesity, there is an obvious need

for research into the long-term consumption of sugar and its effects on brain inflammation which can contribute to cognitive dysfunctions.

2.2 Feeding and Olfaction

Food intake relies on homeostatic regulation and hedonic sensations, with olfaction largely driving food choice as a key sensory modality for assessing the hedonic value of food (Palouzier-Paulignan et al., 2012). The appetite controlling hormones and modulators are highly integrated in the olfactory bulb (OB), olfactory mucosa (Palouzier-Paulignan et al., 2012) and the olfactory cortex (Caillol et al., 2003; Getchell et al., 2006; Hill et al., 1986; Tong et al., 2011), as there are high concentrations of their signalling molecules and receptors present in these areas (Palouzier-Paulignan et al., 2012). Some of these modulators include insulin, ghrelin, leptin, neuropeptide Y and cholecystokinin (Brunert & Rothermel, 2021; Konishi et al., 2017). These hormones also work to modulate olfactory activity. Orexigenic hormones such as ghrelin and orexins, which have maximal levels before meals, enhance olfactory performance (Baier et al., 2008; Bayard et al., 2010; Tong et al., 2011) to aid food localization. Fittingly, anorexigenic molecules such as insulin and leptin decreases smelling abilities and induce satiety-related behaviors (Getchell et al., 2006; Guthoff et al., 2009; Ketterer et al., 2011), such as food avoidance. Olfaction is also closely related to the autonomic regulation of the digestive organs as it is required to prepare the digestive tract for food intake (Powley, 2000). Anatomically, as demonstrated through Figure 1, olfactory information is carried from the OB to the hypothalamus, the primary neurological structure for appetite control (Challet, 2019), through a multi-synaptic pathway. Together, this information shows how important olfaction is for mediating appetite.

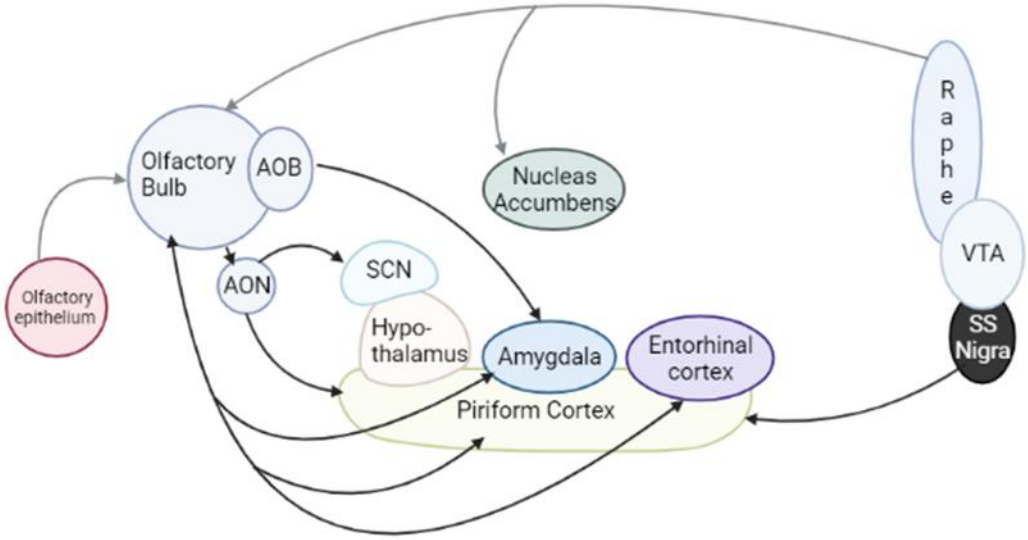

Figure 1: Diagram of Olfactory Circuitry

Black arrows indicate efferent projections and double-headed black arrows indicate two-way communication. Grey arrows indicate centrifugal input to the olfactory bulb. AOB = accessory olfactory bulb, AON = Anterior olfactory nucleus, Raphe = dorsal and median raphe nuclei, SS nigra = substantia nigra, SCN = suprachiasmatic nucleus, VTA = ventral tegmental area. Modified from Kelly, Wrynn, and Leonard (1997), and Krout et al. (2002) and Palouzier-Paulignan et al. (2012). Created with BioRender.com

When investigating obesogenic diets on the brain, it is important to look at the effect of obesity on the appetite-related neurological structures. As mentioned previously, the hypothalamus is the primary appetite controlling centre in the brain (Challet, 2019). It regulates appetite through receiving peripherally derived hormones, such as insulin or ghrelin (Palouzier-Paulignan et al., 2012) to initiate a hormone cascade, to cause feelings of hunger or satiety, which influences the individual to act accordingly (Challet, 2019). It has been found that if an individual were to consume an obesogenic diet, the hypothalamus would become inflamed (Chen et al., 2021; Dorfman & Thaler, 2015; Gao et al., 2017; Lainez et al., 2018). This changes the hypothalamic feeding pathways and causes insulin and leptin resistance within the hypothalamus, dysregulating its ability to supress hunger and feeding and further contributing to a high-caloric intake and weight-gain (Miller & Spencer, 2014; Thaler & Schwartz, 2010). This information highlights the importance of investigating the effect of obesogenic diets on appetite-related brain structures, including the olfactory

bulb. The effect of high-sucrose consumption on the olfactory system requires further investigation. The olfactory bulb is also suitable candidate for obesity research as the olfactory bulb continually receives new neurons throughout life to replenish certain neuron populations (Obernier & Alvarez-Buylla, 2019), and it has been found recently that sucrose consumption may affect the post-natal production of neurons (Beecher, Alvarez Cooper, et al., 2021). Altogether, this information shows that the olfactory system is a viable candidate for investigating the effect of sucrose consumption on the brain as it is both appetite-related and has neurogenic properties.

2.3 Neurogenesis

Neurogenesis is the process which involves the production of neurons from progenitor cells. During embryonic development, specialized cells called radial glia undergo neurogenesis to form the neurological structures of the central nervous system (CNS) and the peripheral nervous system (Urbán & Guillemot, 2014). However, after birth, very few neurogenic niches of the brain persist to continually produce neurons (Götz & Huttner, 2005; Urbán & Guillemot, 2014). The production of neurons which occurs postnatally is given the name adult neurogenesis and has been researched extensively in murine models in the two main neurogenic niches: the dentate gyrus of the hippocampus and the subventricular zone (SVZ; Lalli, 2014). The presence of adult neurogenesis in humans was first depicted in 1998 through the use of bromodeoxyuridine injection, which demonstrated the presence of newly generated neurons in the dentate gyrus and the SVZ (Eriksson et al., 1998). Various studies using immunohistochemical techniques and ^{14}C dating have provided a strong case for adult neurogenesis in humans (Boldrini et al., 2018; Ernst et al., 2014; Kempermann et al., 2018). However, the presence of adult neurogenesis in the human brain has remained a controversial topic with significant evidence against the notion of adult neurogenesis

in humans (Abbott & Nigussie, 2020; Sorrells et al., 2021). For example, a recent study showed that hippocampal neurogenesis steeply declines before birth and drops to undetectable levels after 13 years of age in humans (Sorrells et al., 2018). Subventricular neurogenesis in humans seems to have similar trends, with robust neurogenesis in infancy followed by a steep decline after two years of age (Coletti et al., 2018; Paredes et al., 2016; Wang et al., 2011). Despite its relatively short appearance in post-natal life, it is worth noting that early post-natal SVZ neurogenesis in humans may be necessary to maintain functional synaptic plasticity, and disruption to this pathway could cause the development of neurological conditions in infancy (Sanai et al., 2011). Given the growing rate of sugar consumption in modern society, and indeed even in baby food (Beal, 2020), there is a need to investigate the effect of sugar consumption on SVZ neurogenesis.

2.3.1 Olfactory neurogenesis

The neurogenesis of olfactory interneurons begins in the SVZ, the largest neurogenic niche in the adult brain (Mirzadeh et al., 2008). Along with ependymal cells, the walls of the lateral ventricles are lined with adult neural stem cells known as B1 cells (Mirzadeh et al., 2008; Obernier & Alvarez-Buylla, 2019; Shah et al., 2018). This layer of cells is regarded as the subventricular zone. The B1 cells hold many similarities to radial glia (Lacar et al., 2011; Lim & Alvarez-Buylla, 2016). The replenishment of olfactory interneurons begins when B1 cells asymmetrically divide to produce transient amplifying intermediate progenitor cells (IPCs, or C cells) (Ortega, Berninger, et al., 2013; Ortega, Gascón, et al., 2013; Rasool et al., 2022; Yadirgi & Marino, 2009). These cells then divide a further three to four times before giving rise to neuroblasts (A cells) primed for migration (Jara et al., 2022; Martoncikova et al., 2014). The A-cells proceed to travel towards the OB from the

SVZ through homophilic chain migration (Martončíková et al., 2021) along specialized structures known as the rostral migratory stream (RMS; Figure 2 A-C). The RMS is vital for optimizing neuroblast travel to the OB as it is constituted of a meshwork of structurally supportive astrocytes and blood vessels (Angelidis et al., 2018; Martončíková et al., 2021). Once the neuroblasts have arrived at the OB, they detach from the chains and migrate radially towards their target destination where they will differentiate into various types of olfactory interneurons and integrate into the existing olfactory circuitry (Alfonso et al., 2015; Obernier & Alvarez-Buylla, 2019).

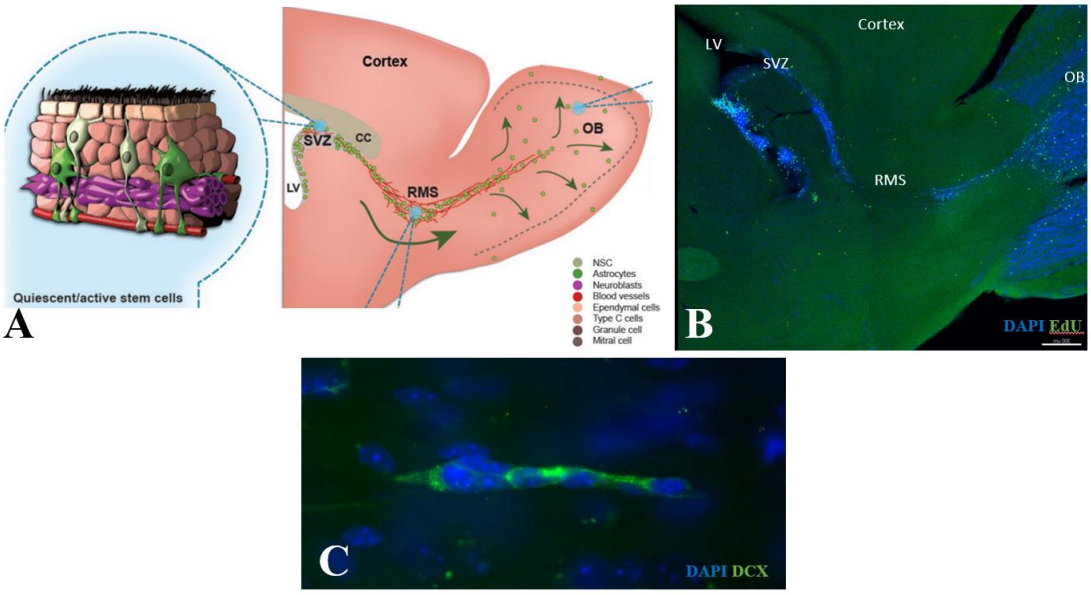

Figure 2: Depictions of neuroblast migration from the subventricular zone through the rostral migratory stream to the olfactory bulb.

A) Schematic diagram of the Subventricular zone, rostral migratory stream and olfactory bulb (CC = corpus collosum, LV = lateral ventricle, OB = olfactory bulb, RMS = rostral migratory stream and SVZ = subventricular zone). Adapted from Gengatharan et al. (2016). **B)** Confocal image of a sagittal section of mouse brain that has been labelled with 5-Ethynyl-2-deoxyuridine (EdU) to label proliferative cells in the subventricular zone, rostral migratory stream and the olfactory bulb. The green nuclei are EdU positive cells, and the blue is 4',6-diamidino-2-phenylindole (DAPI). The scale bar is 300 µm. **C)** A small collection of neuroblasts labelled with doublecortin (green) and DAPI (blue) indicates homophilic chain migration.

It is worthy to note that the B1 cells have an element of heterogeneity depending on their location within the SVZ, which influences the type of olfactory interneurons the adult stem cells may produce (Fiorelli et al., 2015; Mizrak et al., 2019). The walls

of the lateral ventricle contain adult stem cells, however the SVZ is regarded as being regionally specific in the interneurons they give rise to. Refer to Figure 3 for a visual representation of some examples of different types olfactory interneurons and their regions of origin in the SVZ. The B1 cell heterogeneity is specific to the cells themselves and do not occur as a result of their respective location as they are highly resilient to changes in cell fate. This is shown when transplanting B1 cells from dorsal to ventral regions, and vice versa, had no effect on the types of cells they generated (Merkle et al., 2007).

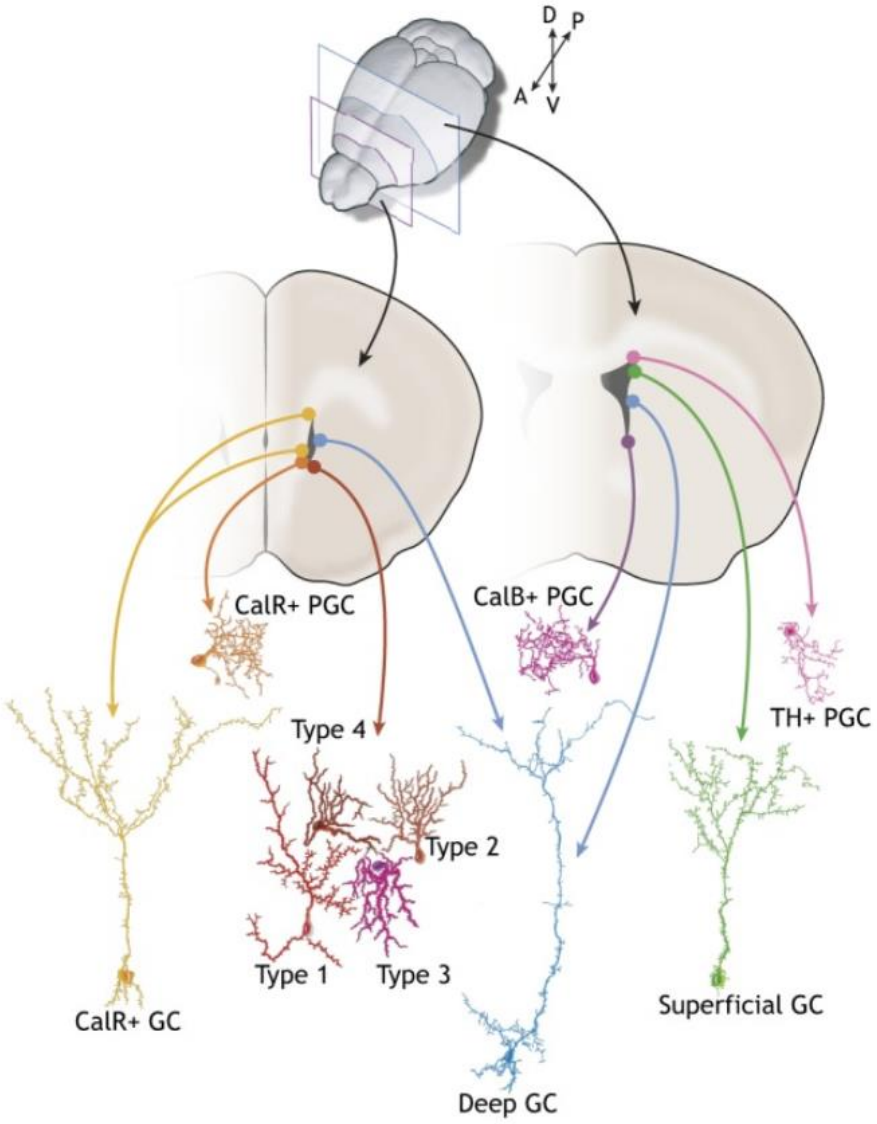

Figure 3: B1 cell heterogeneity

Depending on their location in the SVZ, the B1 cells are region specific in terms of the types of olfactory interneurons they give rise to. This heterogeneity exists along the anterior-posterior and the medial-lateral axis. B1 cells give rise to at least 10 different subtypes of interneurons. The B1 cells located in the posterior dorsal region of the SVZ (indicated in the coronal section on the right) give rise to superficial granule cells (GC; shown in green) and tyrosine-hydroxylase (TH)+ periglomerular cells (PGC; shown in pink). B1 cells of the posterior ventral region produce calbindin (CB)+ PGCs. B1 cells located in the anterior medial region (indicated in the coronal section on the left) generate calretinin (CR) + PGC (shown in orange). The cells of the anterior ventral region of the SVZ gives rise to 4 additional types of interneurons of the granule layer (type 1-4), and a stripe along the ventral surface, which spans across both the anterior and posterior regions, forms deep GC (shown in blue). Image retrieved from Obernier and Alvarez-Buylla (2019).

2.3.2 Olfactory interneurons and their classifications

Once the neuroblasts arrive to the OB, they are now able to differentiate into their predetermined cell fate as olfactory interneurons (Mizrak et al., 2019). Bulbar interneurons will largely inhabit the glomerular layer, as juxtaglomerular cells, or the granular layer, as granular cells. To understand the way in which the OB interneurons relate to the surrounding circuitry, we must first give an explanation to how olfactory information is transduced from the nasal cavity to the OB (Figure 4).

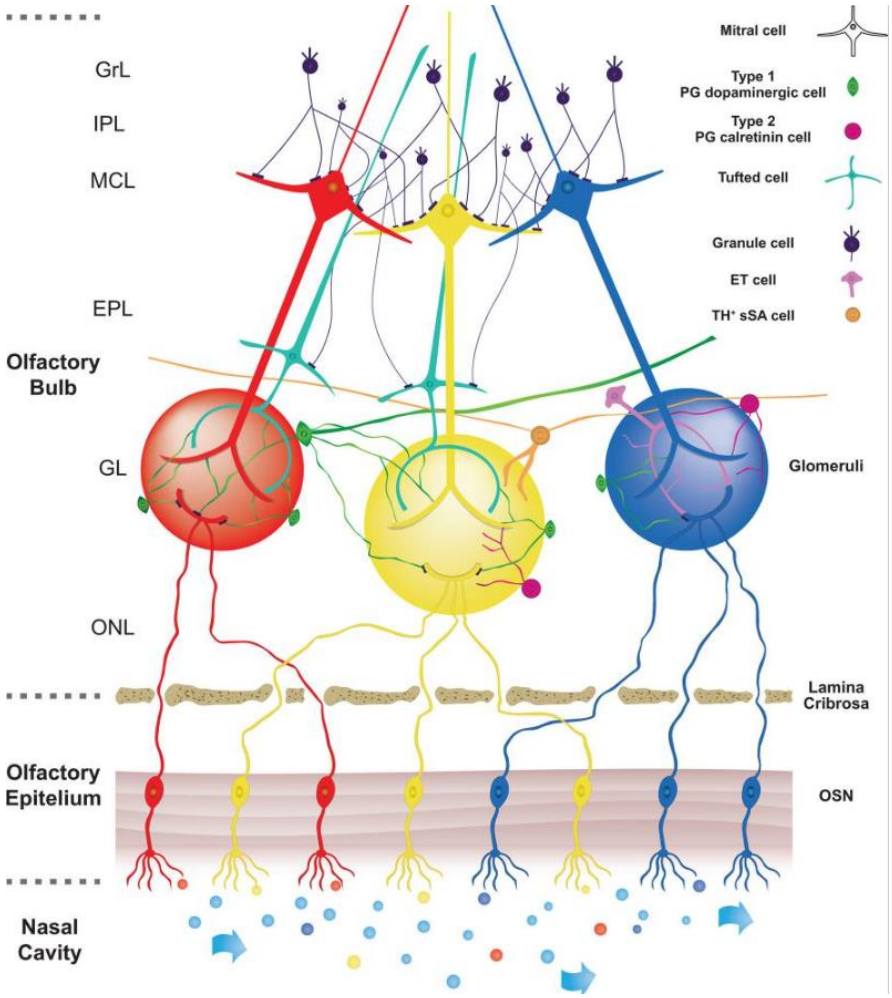

Figure 4: Schematic diagram of the OB circuitry

The circuity of the nasal cavity, olfactory epithelium and OB involved in transducing olfactory information from the olfactory sensory neurons (OSNs) in the nasal cavity to the mitral cells and tufted cells of the OB. A collection of other olfactory interneurons is also involved in this circuit including the juxtaglomerular cells (Type 1 and Type 2 PG cells, ET cells, and TH^+ sSA cells) in the glomerular layer, and the granule cells in the granule layer. ONL = olfactory nerve layer. GL = Glomerular layer. EPL = External plexiform layer. MCL = Mitral cell layer. IPL = Internal plexiform layer. GrL = Granule layer. PG = Periglomerular. ET = External tufted. TH = Tyrosine hydroxylase. sSA = Superficial short axon. Image retrieved from Capsoni et. al (2021).

Olfaction begins in the nasal cavity, where odorant molecules bind to the receptors of olfactory sensory neurons (OSN) which are located in the olfactory epithelium (Capsoni et al., 2021). The OSNs then transduce the odorant information through the lamina cribrosa and into the OB, where their axons will travel through the olfactory nerve layer (ONL) and terminate in their designated glomeruli in the glomerular layer (GL) (Tufo et al., 2022). The OSNs which express the same odorant receptor will each terminate in the same corresponding glomerulus, as shown through the colour coded OSN and glomeruli. The OSN terminals make a synapse with the dendrites of the OB projection neurons: mitral cells and tufted cells. These neurons transduce the olfactory information to other cortical structures for high order olfactory processing (Mori et al., 2013; Nishizumi et al., 2019). At the level of the glomerulus there are a number of juxtaglomerular neurons. Figure 4 makes note of external tufted (ET) cells, short surface axon (sSA) cells, and type 1 and type 2 periglomerular (PG) cells. All of these cells make synaptic connections with other neurons in the glomerular region, such as the OSNs, projection neurons or other interneurons (Capsoni et al., 2021). The cell bodies of the tufted cells are located in the external plexiform layer (EPL), whereas the cell bodies of the mitral cells are located in the mitral cell layer (MCL). The granule cells are another type of olfactory interneuron, and their cell bodies are located in the granule cell layer (GrL), they also make synaptic connections with the projection neurons (Takahashi et al., 2018).

The interneurons of the OB are largely GABAergic (Burton, 2017; Parrish-Aungst et al., 2007), meaning that their overall role in the OB is mainly to enforce inhibition on the surrounding circuitry. More specifically, interneurons use lateral and recurrent inhibition to closely regulate the activation of the olfactory projection

neurons to allow for a more synchronised stimulation of the olfactory cortex (Burton, 2017; Matsuno et al., 2017; Najac et al., 2015; Schoppa & Urban, 2003). Olfactory interneurons have been found to aid in olfactory cognition as they are directly involved with functions such as odour detection and value judgement of odour information, as well as long-term odour memory (Lazarini et al., 2009; Sakamoto et al., 2014). They are also highly active during difficult sensory discrimination tasks (Wu et al., 2020). Both juxtaglomerular cells and granule cells can be further categorised via morphological features and their immunoreactivity.

The glomerular layer of the OB contains three main anatomical subdivisions of juxtaglomerular cells: external tufted (ET) cells, short surface axon (sSA) cells, and periglomerular (PG) cells (Capsoni et al., 2021; Pinching & Powell, 1971). ET cells can be further subdivided based on the presence, or absence, of secondary dendrites (Macrides & Schneider, 1982; Schoenfeld et al., 1985). The subpopulation with secondary dendrites is the more common of the two, and are mostly observed closer to the border between the GL and the EPL (Nagayama et al., 2014). sSA cells can be identified through their long interglomerular axons, which interconnect a variable number of glomeruli (Kiyokage et al., 2010). For example, a single sSA cell can have an axon of up to 1 mm in length, with its dendrites innervating up to 50 glomeruli (Capsoni et al., 2021). PG cells are characterised through their lack of axons, extensive dendritic arborisation and a small soma diameter (Batista-Brito et al., 2008; Fogli Iseppe et al., 2016), and they mostly innervate only one glomeruli (Kiyokage et al., 2010; Pinching & Powell, 1971). They can be further characterised into two different types depending on whether they synapse with OSNs (Type 1) or not (Type 2; Kosaka & Kosaka, 2007; Shao et al., 2009). ET cells, sSA cells and type 1 PG cells are all immunoreactive to tyrosine hydroxylase (TH), the enzyme responsible for the rate

limiting step of dopamine synthesis (Capsoni et al., 2021; Kaushik et al., 2007). Type 2 PG cells are immunoreactive for calbindin and calretinin (Kosaka & Kosaka, 2007; Nagayama et al., 2014), which are calcium binding proteins often used as a general cell marker for identification purposes. Expression of TH, calbindin and calretinin in periglomerular cells is mutually exclusive, further characterising them as different subtypes.

Olfactory interneurons are also present in the granule layer of the olfactory bulb. The granule cells have a variety of subpopulations, which have been categorised based on the location of their cell body, their connectivity with the surrounding environment and their expression of calretinin (Fernández Acosta et al., 2022; Lim & Alvarez-Buylla, 2014). The more common subtypes of granule cells are type-I, type-II, type-III, type-IV (otherwise referred to as deep-branching), type V (otherwise referred to as shrub) and type-S (Merkle et al., 2014; Naritsuka et al., 2009; Orona et al., 1983).

It is important to reiterate that the olfactory interneurons are largely inhibitory to the surrounding circuitry, as 95% of the interneurons are GABAergic (Burton, 2017; Parrish-Aungst et al., 2007). This includes the dopaminergic interneurons as 97% of them are also GAD67+ (Kiyokage et al., 2010), making them DAergic-GABAergic neurons.

Although there are different ways of classifying interneurons, for this research project, they will be defined by their immunoreactivity.

2.3.3 Factors Affecting Neurogenesis

While adult neurogenesis persists throughout life, many factors can alter its effectiveness. Aging is known to cause reduced neurogenesis in the SVZ (Jin et al., 2003). Mastication has been shown to play an important role in optimal SVZ proliferation as a soft diet impairs neurogenesis of the SVZ (Noguchi et al., 2017;

Utsugi et al., 2014). This diet caused a decrease in neurogenic cell migration to the OB which impaired olfactory cognitive functions such as avoidance of unpleasant odors (Noguchi et al., 2017). Vitamin C deficiency has been found to reduce SVZ neurogenesis and proliferation in guinea pigs (Jara et al., 2022). Maintaining physical activity has been consistent with enhanced SVZ neurogenesis and the number of functionally active neurons in the OB (Nicolis di Robilant et al., 2019). Fructose consumption has been found to impair hippocampal neurogenesis (Cisternas et al., 2015; Fierros-Campuzano et al., 2020; van der Borght et al., 2011). Long-term hyperglycaemia induced by increased glucose consumption, in a rat model of Type 2 diabetes, is reported to increase neurogenesis in both the SVZ and hippocampus, however, lower survival rates of the newborn cells followed as a result (Lang et al., 2009). Recently, our lab also found that long-term sucrose consumption affects the hippocampal neurogenesis which caused deficits in spatial and episodic memory (Beecher, Alvarez Cooper, et al., 2021). However, it remains unknown whether long-term sucrose consumption also affects other adult neurogenic areas including the SVZ and the OB.

2.4 Neuroinflammation

In a healthy brain environment, neuroglia are integral in maintaining brain homeostasis by providing a range of supporting functions. Astrocytes perform an array of neurosupportive tasks including their role in forming the blood-brain barrier (Serlin et al., 2015). Microglia are distinct for their myeloid origin and are designed to phagocytose debris within the CNS (Ginhoux et al., 2010). While these cell types are supportive under healthy conditions, they often exacerbate CNS insults, and thus, contribute to neuroinflammation (Guillamón-Vivancos et al., 2015).

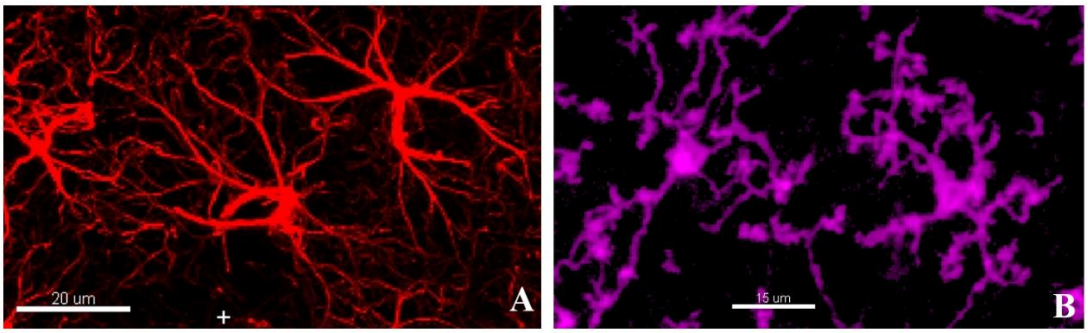

Figure 5: Confocal images of neuroglial cells
(A) The sagittal section of the hippocampus showing astrocytes immunolabeled with GFAP and microglia with TMEM119 (B). Scale bar is 20 µm for (A) and 15 µm for (B).

2.4.1 Astrocytes

Under healthy conditions, astrocytes are characterized by a small bulbous soma with an array of thin and distinct processes called branches with further secondary and tertiary branches known as branchlets (Figure 5A; Khakh & Sofroniew, 2015). Astrocytes have a range of structures that help to optimize overall brain function. They have a specific cellular process called an astrocytic end foot which interacts with a cerebral blood vessel and helps to form the blood-brain barrier (BBB; Kubotera et al., 2019). The astrocytic end feet closely control the diffusion of substances such as nutrients and gasses between the brain parenchyma and systemic circulation to maintain brain homeostasis (Johnsen et al., 2017; Loiola et al., 2021). They also regulate the blood flow to the surrounding brain tissue by controlling blood vessel dilation and constriction (Kubotera et al., 2019; Quintana, 2017). Peri-synaptic astrocytic processes encapsulate neuronal synapses (Khakh & Sofroniew, 2015) to prevent diffusion of neurotransmitters to the extracellular space thus preventing unwanted accessory neuronal activation. They also uptake synaptic ions and neurotransmitters to maintain synaptic homeostasis (Stogsdill et al., 2017; Zhou et al., 2019). This intricate relationship between astrocytes and neurons shows how astrocytes regulate synaptic connection and contribute to synaptic plasticity (Ma et al., 2016; Zhou et al., 2019).

Astrocytes respond to all forms of CNS injury and will undergo a process called reactive astrogliosis (Guillamón-Vivancos et al., 2015). The astrogliosis is not merely a binary state of activation, rather a spectrum of changes that may occur to their morphology and molecular expression (Escartin et al., 2021). In the instance of severe injury to the CNS, increased astrocytic proliferation and hypertrophy have been reported (Sofroniew, 2009). The astrocytic branches may also lengthen, overlap, and interdigitate with those of other astrocytes, causing long-term alterations to the neural tissue architecture known as a glial scar (Guillamón-Vivancos et al., 2015). This is important as the glial scar isolates the site of injury to prevent the spread of neuroinflammatory markers and the arrival of additional inflammatory cells, thus helping to restrict the extent of neuroinflammation (Guillamón-Vivancos et al., 2015). However a glial scar will also act as a physical barrier for axonal regeneration and cellular migration, making it nearly impossible to restore the tissue after the initial injury (Rodríguez-Gómez et al., 2020; Sofroniew, 2009).

As mentioned, astrocytes are integral in maintaining a functional neurological environment. They are also essential in neuroblast migration along the SVZ and RMS (Lalli, 2014). Structurally, the RMS utilizes a scaffold of blood vessels and an 'envelope' of astrocytes, commonly referred to as a glial tube (Fujioka et al., 2019), to serve as a physical substrate for neuroblast migration (Bozoyan et al., 2012; Martoncikova et al., 2014). The astrocytes of the RMS line the blood vessels in a parallel manor (Fujioka et al., 2019), adopt a polarized appearance instead of the characteristic stellate shape (Whitman et al., 2009) and use their processes to interdigitate with the migrating neuroblasts (Martončíková et al., 2021). Refer to Figure 6 which shows the bipolar appearance of RMS astrocytes. The neuroblasts can also release a diffusible protein which repulses astrocyte processes, enabling the

neuroblasts to remodel the astrocytic scaffold and move through the RMS (Kaneko et al., 2010; Peretto et al., 1999). Interestingly, electron-microscopy has demonstrated that neuroblasts in the RMS can make direct contact with blood vessels without any astrocyte or pericyte involvement (Peretto et al., 2005; Whitman et al., 2009). In a similar manor, B1 cells and C cells of the SVZ can make direct contact with the blood vessels at sites devoid of astrocyte or pericyte coverage (Tavazoie et al., 2008; Zhang et al., 2014), a unique modification to the blood brain barrier specific to the SVZ. In the case of the SVZ, the resident neural stem cells may be exposed to direct contact with blood vessels without any protection from the blood brain barrier. This is especially interesting considering the blood vessels of the SVZ have been found to have a lower permeability (Colín-Castelán et al., 2016), indicating that plasma-infused molecules may be able to diffuse into the SVZ with more ease than in other parts of the brain. Both of these findings imply that the stem cells of the SVZ experience a higher exposure to blood-borne molecules, including those with higher molecular weights (Colín-Castelán et al., 2016; Tavazoie et al., 2008).

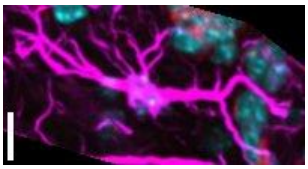

Figure 6: An isolated astrocyte of the RMS

A confocal image of an astrocyte of the RMS with its processes arranged in a bipolar manor instead of the typical star shape. Astrocyte immunolabeled for glial fibrilliary astrocytic protein (GFAP) in magenta and DAPI in cyan. Scale bar is 10 µm.

Not only do astrocytes serve the structural integrity of the RMS but they also have been proposed to aid in the vasophilic migration of neuroblasts through the RMS (Bovetti et al., 2007; Snapyan et al., 2009). In 2009, the Saghatelyan group proposed a molecular pathway utilizing bone-derived neurotrophic factor (BDNF) as a mechanism for neuroblast migration (Snapyan et al., 2009). The endothelial cells of

the blood vessels in the RMS produce BDNF which binds to p75NTR, a low-affinity receptor for BDNF expressed on neuroblasts, causing the neuroblasts to enter the 'migratory phase' in which the cell body will 'leap' to the end of their leading process.

2.4.2 Microglia

Microglia are another type of glial cell that are crucial for maintaining CNS homeostasis. Microglia originate from a myeloid lineage, making them the resident immune cells of the CNS (Ginhoux et al., 2010; Graham et al., 2016). In this role, microglia play a crucial part in initiating an inflammatory response to CNS injury. They take part in phagocytosing cellular debris and foreign cells while also releasing crucial mediators which recruit microglia and other glial cells (Siddiqui et al., 2016; Tremblay et al., 2011). Furthermore, microglia have roles in regulating neural tissue such as synaptic pruning; whereby microglia will phagocytose unused or dysfunctional synapses (Kettenmann et al., 2013). This is a task mainly undertaken during development, however, it persists throughout adult life (Cornell et al., 2021).

Microglia in the healthy CNS show a ramified phenotype with numerous ramified processes extending from their cell body (Figure 5B); these processes undergo dynamic behaviour and are continuously monitoring their environment (Colonna & Butovsky, 2017; Tang & Le, 2016; Zhou et al., 2019). Under pathological conditions, the phenotype of microglia rapidly changes, and they transform from a ramified morphology to an amoeboid morphology (Colonna & Butovsky, 2017; Tam & Ma, 2014). Amoeboid microglia have enlarged cell bodies with shorter cell processes.

Microglia have been found to have specialized roles in the SVZ/RMS. The blood vessel scaffold and astrocytic envelope of the adult RMS do not develop until several weeks postnatally (Bozoyan et al., 2012; Law et al., 1999). Instead, the early postnatal

RMS is supported by ameboid-shaped microglia which line the RMS borders prior to the development of the characteristic blood vessel and astrocytic features (Meller et al., 2023). These microglia were found to undergo homeostatic maintenance of the RMS by controlling the domain of the early postnatal RMS through phagocytosing any "excessive" neuroblasts and apoptotic cells (Meller et al., 2023). The microglia of the adult SVZ/RMS/OB have been found to have a distinct morphology, in that, they display an enlarged cell body with relatively few and notably thick processes (Ribeiro Xavier et al., 2015). Vastly different from their counterparts in the cerebral cortex which are regarded for their smaller cell bodies and highly ramified processes (Ribeiro Xavier et al., 2015). Normal and healthy microglia of SVZ/RMS also have a lower expression of P2RY12 than the microglia of surrounding areas (Ribeiro Xavier et al., 2015). P2RY12 is a purine receptor which has been associated with microglial process extension and is found to have a high expression during a normal homeostatic state and a markedly lower expression in reactive microglia (Haynes et al., 2006; Hua et al., 2023). When noting that there is evidence to suggest that purine signaling promotes the proliferation of type A and type C cells in the RMS (Suyama et al., 2012). Riberio Xavier et al. speculate that the microglia of the RMS/SVZ may have a lower resting P2RY12 expression so as to avoid inappropriate activation in response to locally purigenic mitogens (2015). Microglial P2Y12 signaling has been found to regulate neurogenesis in the SVZ from post-natal day 1 (Cserép et al., 2022), and promote proliferation in the adult mouse SVZ (Suyama et al., 2012). Altogether, this information shows that the microglia of the SVZ and RMS are highly specialized cells which specifically aid in the normal neurogenic function of the SVZ and RMS.

2.4.3 Diet and Neuroinflammation

Pathological glial activity has been linked to the development of disease states such as Parkinson's disease, Huntington's disease, Alzheimer's disease and multiple sclerosis (Brambilla, 2019; Joers et al., 2017; Long & Holtzman, 2019; Sellgren et al., 2019). Similarly, correlations between pathological glial activity and obesogenic diets have been observed. High-fat diets have been shown to initiate neuroinflammation in the hypothalamus, through activation of both astrocytes and microglia (Chen et al., 2021; De Souza et al., 2005; Dorfman & Thaler, 2015; Horvath et al., 2010; Lainez et al., 2018). In a similar way, high sugar and fat diets can cause increases in hypothalamic neuroinflammation (Gao et al., 2017). It has been shown that microglial (mouse model) activity in the hypothalamus greatly influences energy homeostasis, as reduced hypothalamic microgliosis causes hypophagic behavior and conversely, inducing hypothalamic microgliosis resulted in hyperphagic behavior and weight gain (Valdearcos et al., 2017). This is significant as it establishes hypothalamic neuroinflammation as a mediator of dysregulated energy balance.

The current literature on the inflammatory effect of sugar consumption is conflictive. An *in vitro* model demonstrated that when exposed to sugar, microglia would react to stimuli that they normally ignore (Zhang et al., 2015). Fructose overconsumption in rats can cause neuroinflammation (Djordjevic et al., 2015). Whereas others have found that a high-fructose diet could not induce signs of neuroinflammation, however, cognitive deficits were evident (Beilharz et al., 2016). It is worth noting that differences in species and experimental design could be the cause of these discrepancies. Further, different types of sugar such as high-fructose corn syrup, fructose or sucrose also showed discrepancy in the amount of neuroinflammation in animal models (Hsu et al., 2015; van der Borght et al., 2011).

Long-term consumption of a 5% sucrose drink was also found to reduce the number of microglia in the dentate gyrus of the hippocampus (Beecher, Wang, et al., 2021). Together this information proves that there is a need to investigate more into the reaction of glial cells in response to long-term sugar consumption to indicate the neuroimmune status of brain parenchyma.

2.5 Research Problem

As obesity is becoming more prevalent in society, it is important to identify any pathological neurobiology that may occur as a result of obesogenic diets. Obesity is an inflammatory disease which can cause neuroinflammation in the hypothalamus, a crucial structure for appetite control (Challet, 2019). We have shown that long-term sucrose consumption caused gliosis in the hippocampus (Beecher, Alvarez Cooper, et al., 2021), however it remains unclear whether the obesogenic diet of long-term sucrose consumption will cause neuroinflammation in other brain structures closely related to appetite, such as the OB. Forebrain adult neurogenesis is important to regulate brain function. Our lab recently found that hippocampal neurogenesis (which is essential for memory) was reduced after long-term sucrose consumption, causing memory deficits (Beecher, Alvarez Cooper, et al., 2021). However, it is currently unknown if long-term sucrose consumption affects other neurogenic niches of the brain, such as the SVZ and the OB. Subventricular neurogenesis is especially relevant to diet regulation as it constantly replenishes the neurons of the OB which has an important role in appetite control through its neural pathways to the hypothalamus, and its high integration of appetite-controlling hormones.

Chapter 3: Research Design

3.1 Ethics Statement

All procedures and protocols involving the use of mice were approved by The University of Queensland and The Queensland University of Technology Animal Ethics Committees (approval number: QUT/053/18). All experimentation was undertaken in accordance with the *Animal Research Act 2001* (Qld), the associated *Animal Care and Protection Regulation 2012* (Qld) and the Australian Code for the Care and Use of Animals for Scientific Purposes, 8th Edition.

3.2 Overview of Methodology and Timeline

Two groups of animals (n = 4/group) were used to investigate the aims of this thesis. Based on the previous work from the laboratory (Beecher et al, 2021), where sucrose consumption produced a 20% change in neurogenesis, G*power (Dusseldorf University, Germany) power calculations using G*power software (Dusseldorf University, Germany) suggest that to observe a significant difference of 20%, with a large effect size of 0.8, using a two-tail student t-test, a total sample size of minimum 15 animals within 2 groups (n = 8/group) is needed. Hence, as a pilot study, this investigation includes 4 animals/group to establish the feasibility of this study. This limitation is discussed further in Chapter 6.

Figure 7 provides an overview of the experimental techniques used to help investigate the effects of *ad libitum* access to sucrose on olfactory neurogenesis and neuroinflammation.

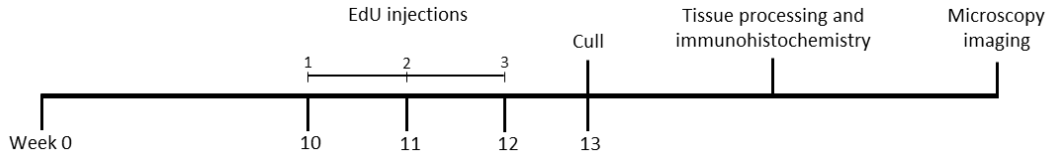

Figure 7: Timeline of experimental techniques

The animals were treated with *ad libitum* access to either sucrose or water (control) from week 0, which continued throughout the course of animal housing. The mice received three EdU injections to label proliferative, cells and were harvested during week 13. Tissue processing and immunohistochemistry and microscopy imaging were then completed on the extracted brain tissue.

3.3 Animals and Housing

Five-week-old male C57BL/6J mice were delivered and housed at the Pharmacy Australia Centre of Excellence (PACE) for one week of acclimatisation prior to experimentation. The mice were kept under reversed light cycle conditions (room lit between 9pm-9am) with climate control with *ad libitum* access to food and water. Mice were weighed twice a week for welfare checks, and to record their weight gain.

3.4 Sucrose Consumption Models

After one week of habituation, the mice were housed separately and were made subject to a modified two bottle choice model with continuous access to either water (control group) or 25% sucrose (w/v; treatment group). The sucrose/water was presented in 50 mL plastic falcon tubes fitted with rubber stoppers and a 6.35 cm stainless-steel sipper tube with double ball bearings. The bottles were weighed and refilled twice a week to track sucrose consumption.

3.5 EdU injection, tissue harvesting and immunohistochemistry.

Following 10 weeks of sucrose consumption, the mice were subjected to three injections of the cell proliferation marker, 5-ethynyl-2´-deoxyuridine (EdU; 50 mg/kg intraperitoneal) over two weeks at days 0, 7 and 15 (Figure 7) as previously described (Belmer et al., 2018; Patkar et al., 2019). EdU is used to label all actively dividing

precursor cells in the SVZ, RMS and the OB. One week after the last EdU injection, the mice were anesthetized with sodium pentobarbital (100 mg/kg, Lethabarb, Virbac, Australia) and transcardially perfused with 4% (w/v) paraformaldehyde (PFA). Brains were extracted and post-fixed overnight in 4% PFA (w/v) at 4^{o}C. The brains were divided into hemispheres, embedded in 5% agar and sectioned into sagittal sections of 40 µm thickness using a vibratome in 0.1 M phosphate buffer saline (PBS). The sections for each hemisphere were stored in 0.02% sodium azide in PBS. The sections containing the RMS and SVZ were found through preliminary 4′,6-diamidino-2-phenylindole (DAPI) staining. In total, every stain had 1-5 sections from 2-4 animals per group. Sections were rinsed in 1X PBS initially, then incubated in 1:1000 solution of DAPI in 1X PBS for 5 mins followed by rinses in 1X PBS. Initial optimisation methods showed that all immunolabelling combinations were efficient when the EdU Click-iT™ assay was performed before the immunohistochemical techniques. Therefore, the sections were permeabilised in 1X PBS containing 1% Triton and 0.1% Tween for 30mins at room temperature. Then, the sections were washed in an EdU blocking solution of 3% (w/v) Bovine Serum Albumin (BSA) and 0.3% (v/v) Triton X100 in 1X PBS prior to 30 min incubation in the EdU Click-iT™ assay according to the EdU Click-iT™ EdU Alexa Fluor™ 488 Imaging Kit (Thermo-Fisher Scientific, C10637). Sections were rinsed in EdU blocking then 1X PBS, marking the completion of EdU staining and the commencement of the immunohistochemical stains. Depending on the type of the primary antibody, the sections would then undergo antigen retrieval to further expose the antigens and allow for better staining in a mixture of 10mM of sodium citrate and 0.05% (v/v) tween-20 (pH 6) at 80^{o}C for between 5-15 mins. Sections were then brought back to room temperature in the sodium citrate then washed in 1X PBS and incubated for 1 hour in

immunohistochemical blocking (2% (v/v) normal goat serum/normal donkey serum, 0.3% (v/v) Triton X100 and 0.05% (v/v) Tween-20). The primary antibodies for Calbindin, Calretinin, and TH were used to label the interneurons of the OB. OMP was used to label the olfactory axons in nerve fibre and glomerular layers of OB. Primary antibodies against DCX, GFAP, Ki-67 and Nestin were all used to label the neurogenic cells of the SZV and RMS. DCX is a microtubule-associated protein expressed by immature neurons (Type A cells), Ki67 is a general proliferative marker expressed in cells that divided shortly prior to death of the specimen. Nestin is an intermediate filament protein expressed in dividing neural stem cells (B1 cells). Glial fibrillary acidic protein (GFAP) is expressed by both astrocytes and early-stage neural stem cells (B1 cells). Antibodies against TMEM119 were used to stain for microglia. The sections were incubated in the primary antibodies overnight at room temperature on an orbital shaker (sections labelled with Nestin required a second 'overnight' period at 4 ^{O}C). The next day, the sections were rinsed in immunohistochemical blocking then incubated for 2 hours in an associated secondary antibody solution. If an antibody required a biotinylated secondary, the sections would then be incubated in streptavidin-CY3 in PBS for 30 mins at room temperature followed rinses in PBS. Sections were then mounted with Prolong gold antifade mountant (Thermofisher Scientific, #P10144).

Table 1: Antibodies and concentration used to label different cellular populations associated with olfactory neurogenesis and neuroinflammation

Purpose	Primary Antibodies	Secondary Antibodies
Neurogenic areas (SVZ, RMS)	- Mouse anti-Ki67 (BDPharmingen, 550609, 1:20) - Rabbit anti-DCX (Cell Signalling, A8L1U, 1:500)	- Goat anti-Mouse IgG, Alexa Fluor 594 (Invitrogen, A11032, 1:500) - Goat anti-Rabbit IgG, Alexa Fluor 647 (Invitrogen, A21245, 1:500)
	- Mouse anti-Nestin (Merck, MAB353, 1:500) - Rabbit anti-Ki67 (Abcam, ab15580, 1:250)	- Goat anti-Mouse IgG, Alexa Fluor 594 (Invitrogen, A11032, 1:500) - Goat anti-Rabbit IgG, Alexa Fluor 647 (Invitrogen, A21245, 1:500)
Glial cells/ Neuroinflammation	- Rabbit anti-GFAP (Dako, Z0334, 1:500) - Mouse anti-TMEM119 (synaptic systems, 400011, 1:500)	- Goat anti-Rabbit IgG, Alexa Fluor 555 (Invitrogen, A32732, 1:500) - Goat anti-Mouse IgG, Alexa Fluor Cy5 (Life Technologies, A10524, 1:500)
Olfactory bulb interneurons	- Rabbit anti-Calbindin (Swant, CB38, 1:1500) - Mouse anti-Calretenin (Millipore, MAB1568, 1:500)	- Goat anti-Rabbit IgG, Alexa Fluor 555 (Invitrogen, A32732, 1:500) - Horse anti-Mouse IgG, biotinylated (vector labs, 1:200) + Streptavidin-CY5 (1:1000)
	- Rabbit anti-TH (Abcam, AB152, 1:500) - Goat anti-OMP (WAKO, 544-10001-WAKO, 1:500)	- Donkey anti-Rabbit IgG, Alexa Fluor 568 (Invitrogen, A10042, 1:500) - Donkey anti-Goat IgG, Alexa Fluor 647 (Invitrogen, A32849, 1:500)

3.6 Image acquisition and analysis

3.6.1 SVZ and RMS image acquisition and data collection

The images for all three labelling of the neurogenic areas (Ki67 and DCX, Nestin and Ki67) were acquired via an Olympus FV3000 Laser Scanning Confocal microscope. To commence imaging, a slide would be loaded into the microscope and a 4x map in 401nm would be captured of the sections on the slide to help identify the regions of interest and to ensure uniformity between sections. Three main regions of interest (ROIs) were determined for imaging of the neurogenic labelling (Figure 8A). The ROIs were chosen and named based on Martoncikova et al. (2021). The first ROI

is at the level of the SVZ, the second ROI is at the most proximal part of the RMS where the RMS extends ventrally. This area is known as the vertical arm. The third ROI is at the region where the RMS deviates rostrally to form an angle known as the elbow.

All confocal images taken for analysis were obtained using a 30x oil objective with a depth of 15 µm and a z-step of 0.5 µm (30 z-stacks). These images were then loaded into Huygens Professional v16.10 (Scientific Volume Imaging) for deconvolution to restore volumes without light scattering. The images were deconvolved with a maximum of 50 iterations, with a signal to noise ratio of 1:10 and a quality threshold of 0.001. The deconvolved images were then loaded onto Neurolucida 360 for manual cellular quantification. While only having the DAPI channel active, the maximum projection setting on Neurolucida would be used to define the area of the RMS or SVZ within an image by using the contour function to draw a polygon around the outline of the neurogenic region shown. The surface area of the contour would then be noted for further statistical analysis. The cells quantified within the contour were defined as ‘RMS’ or ‘SVZ’ cells (depending on the location), cells <50 µm outside of either side of the contour were also quantified and defined as ’0-50 µm’ cells. This is visually represented in Figure 8B.

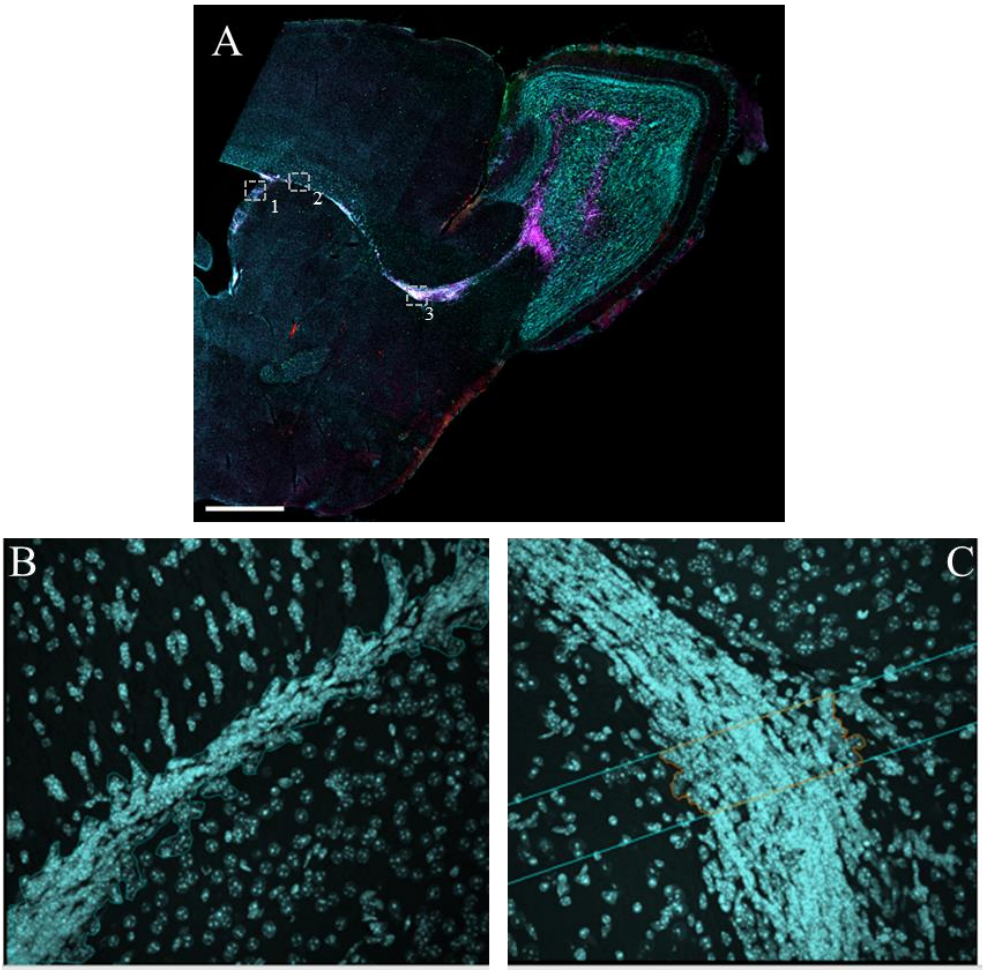

Figure 8: Visual guides for quantification methods

(A) A confocal image of the SVZ and RMS in a sagittal section. Small square boxes have been superimposed on the image to represent the ROIs based on Martoncikova et al. methods (2021). The ROI at the SVZ is depicted (#1), along with the three ROIs of the RMS at the vertical arm (#2), and the elbow (#3). Blue = DAPI, green = EdU, red = Ki67 and magenta = DCX. Scale bar is 300 µm. (B) A confocal image of the vertical arm of the RMS with the DAPI channel. A polygon has been drawn around the RMS (light blue) to allow for manual quantification. (C) A confocal image of the elbow of the RMS with the DAPI channel active. A 50 µm rectangle has been superimposed onto the 'hinge' of the elbow' and a polygon has been drawn around the RMS within the rectangle to allow for manual quantification.

The quantification undertaken at the vertical arm used these techniques to define the ROIs. However, due to the dynamic contours of the SVZ and RMS and the variations of cellular population density, the ROIs at the SVZ and elbow required different quantification techniques.

The SVZ is located along the border of the lateral ventricles, which contain cerebrospinal fluid and are absent of solid tissue. After observing the SVZ images, it

appeared that its boarders would shift in one direction along the X and Y planes as you travelled through the Z-stack. To combat this, a representative region of 10 stacks (5 µm) was chosen for each SVZ image. The chosen region would then be made into a maximum projection image on ImageJ. This image would then be uploaded into Neurolucida, and while only activating the DAPI channel, the contour function would be used to define the borders of the SVZ for the desired quantifiable region. This contour would then be used for quantification on the original image in Neurolucida, while ensuring to only quantify cells within the predetermined representative range of 10 stacks.

The elbow of the RMS is an area far more densely populated with cells than the other parts of the RMS. This is because the elbow of the RMS has a smaller footprint than other parts (eg. the vertical arm) causing the cells to be more densely packed together. This feature makes manual quantification very challenging. To combat this, a premade rectangular contour of 50 µm by 300 µm and placed it over the 'angle' of the elbow in each image, and only quantified within that region. To define the quantified area of the elbow, a maximum projection image would be made and a contour was drawn around the elbow of RMS within the premade rectangle (Figure 8C).

3.6.2 OB interneuron and GFAP TMEM image acquisition and data collection

All sections from the interneuron and neuroinflammatory labelled sections were imaged using an Olympus VS200 Slidescanner on a 20x zoom with a z-step of 1.18 µm (14.16 µm total thickness) at the level of the OB. The GFAP/TMEM sections of the SVZ, RMS and OB were imaged to obtain an insight on the glial cell behaviour in these areas. All images were then opened on QuPath 0.3.0 where the relevant brain

structure was cropped, downsized by 1:2 pixels and exported onto ImageJ, to then be saved as a .tif file.

The data from the CB/CR and Th/OMP stains immunolabelling combinations were all collected using similar techniques. The image would be opened on Neurolucida where 3 ROIs across glomerular layer and 2-3 ROIs in the granule layer were defined using the contour function. Each ROI was composed of 3 glomeruli each. The TH interneurons and the Calbindin interneurons were quantified throughout the whole stack of the 13 images (14.16 µm), except the CR quantification used 5 images because the cells were more defined across this area (4.72 µm).

Due to the obscure morphology of astrocytes and microglia, these cell types were not manually quantified, the primary source of data collection for the GFAP/TMEM119 stain was through Imaris. Firstly, to prepare the images for analysis, each olfactory bulb image was cropped on ImageJ to distinguish two separate layers, the GL and the GrL. This occurred using the polygon selections tool and creating a contour that encompassed the whole of the GL of that image, then using the 'Clear Outside' feature to remove the image surrounding the contour, followed by the 'Crop' feature to fit the cropped image to size which would then be saved as .tif files. This method was applied to all GFAP/TMEM119 images for the GL as well as the GrL. The images were subsequently loaded onto Imaris 8.2.1 (Bitplane) to form 3D reconstructions of the GFAP and TMEM119 labelling ("surface" function in Imaris). These reconstructions were subsequently used for volumetric quantification. The GFAP labelling within the surface was further analysed using the "surface fluorescence statistics" of Imaris to determine the mean fluorescence of each reconstructed surface. The same method was applied for TMEM119 labelling of the GL and GrL images. To determine the total volume of fluorescent labelling in the

image after cropping the ROIs, surface reconstruction of the whole 488 channel was used, by reconstructing the autofluorescence as boundaries of the tissue (Figure 9). The volume of autofluorescence/section was then known to be the volume of the region quantified.

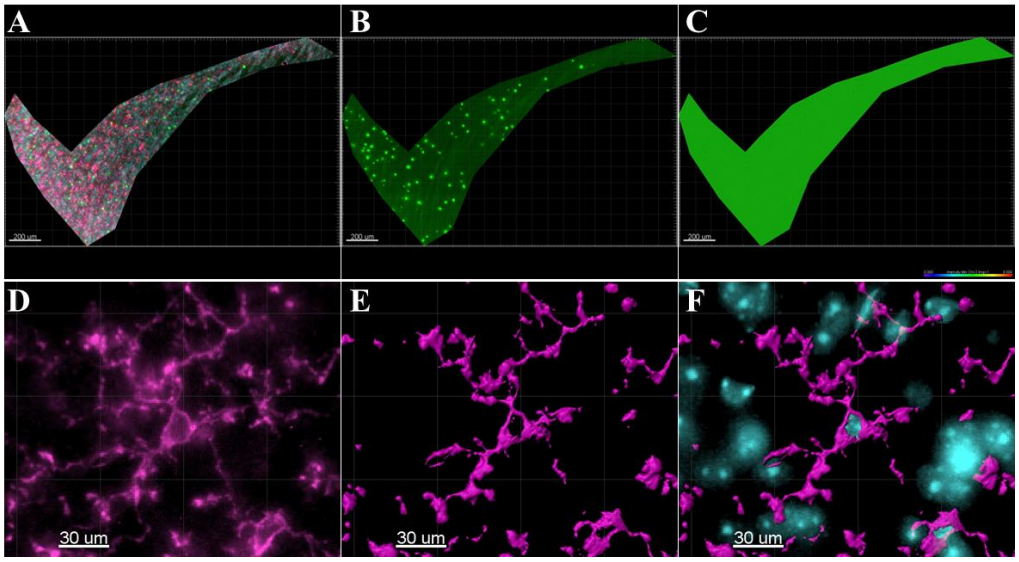

Figure 9: Using Imaris software for reconstructing volumes

(A-C) Acquiring the volume of the ROI in Imaris. (A) A cropped granular layer of an olfactory bulb with all four channels activated. (B) The autofluorescence of the green channel has been exaggerated and using Imaris reconstructions. Using the exaggerated fluorescence, an object was made to encapsulate the whole ROI (C). (D-F) Reconstructing microglia using Imaris. (D) The TMEM119 labelling a microglia. (E, F) Using specific parameters on Imaris, the microglia has been reconstructed.

As detailed previously, there were two sections per animal which had the most lateral section of the RMS/SVZ, and these were included in the GFAP/TMEM stains to observe the glial activity of the SVZ and the subcallosal part of the RMS. Using ImageJ, the SVZ and the RMS of each image were cropped separately as two different ROIs, to then be processed by Imaris in the same way that the GL and GrL of the OBs were analysed.

The amount of EdU colocalization with GFAP and TMEM119 was required at the level of the granule layer of the OB. However, due to the high density of overlapping astrocytes and microglia, these cell types were not able to be counted

individually. Instead, the proportion of EdU colocalising with either one of these cell types was measured using Neurolucida. This was determined by setting three contours in each GrL (in the same locations as the interneuron stains) then counting the number of EdU cells, followed by counting the number of EdU cells that colocalised with either GFAP or TMEM119.

3.7 Statistical analysis

All the obtained data underwent preliminary assortment on Microsoft Excel and were subsequently processed on GraphPad Prism using statistical tests such as 2-way ANOVAs and unpaired t-tests.

Normality tests were conducted to ensure the data was fit for statistical analysis using parametric tests. The following are the tests conducted: D'Agostino & Pearson test, Anderson-Darling test, Shapiro-Wilk test, Kolmogorov-Smirnov test. A data set was considered normally distributed if $p < 0.05$. The results from all tests found that the data was normally distributed.

Table 2: Describing the data derived from Imaris

Measurement	Description	Calculations	Units
Mean [cell type] volume	The average volume of all reconstructed objects	$\frac{Sum\ of\ volumes\ of\ reconstructed\ objects}{Number\ of\ reconstructed\ objects}$	µm^3
Proportion of [cell type] coverage	The proportion of section occupied with reconstructed objects	$\frac{Sum\ of\ volumes\ of\ reconstructed\ objects}{Total\ volume\ of\ section} \times 100$	%
Number of reconstructed cells in 1 mm^3	The number of cells within 1 mm^3 of the ROI	$\frac{Number\ of\ reconstructed\ objects\ in\ ROI}{Volume\ of\ ROI\ (\mu m)} \times 1000000000$	cells
Mean fluorescence per [cell type]	The average mean intensity of reconstructed objects	$\frac{Sum\ of\ the\ mean\ intensities\ of\ reconstructed\ objects}{Number\ of\ reconstructed\ objects}$	iu
Normalised fluorescence	The fluorescence intensity when normalised to the % coverage of reconstructed objects	$\frac{Mean\ intensity}{\%\ coverage}$	iu

Chapter 4: Results

4.1 Long-term sucrose intake increases weight gain.

The effects of long-term unrestricted access to sucrose on body weight. After 12 weeks of *ad libitum* access to 25% sucrose, mice exhibited stable levels of sucrose intake around 80-90 g/kg/day (mean 83.1 ± 1.745 g/kg/day, indicated by the red line; Figure 10A). A significant increase in overall weight was observed, across the 12 weeks of sucrose consumption (Figure 10B', AUC, *p = 0.0391). It can be noted that the sucrose group weights diverge from the water group from week 6 onwards with a significant increase in weight (Figure 10B'', AUC, **p = 0.0070). These results confirm that continuous access to sucrose causes weight gain as it was previously reported in our lab (Beecher, Alvarez Cooper, et al., 2021).

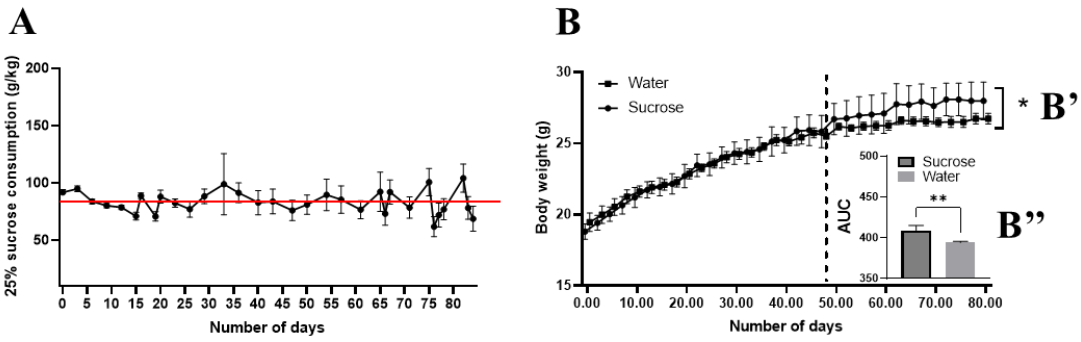

Figure 10: Long-term sucrose consumption causes weight gain.

(A) Mice had *ad libitum* access to a 25% sucrose beverage over the course of 12 weeks and partook in a mean consumption of 83.1 ± 1.745 g/kg/day. (B) The change in body weight of mice over time. (B') The animals subjected to long term sucrose consumption had a significantly increase in weight gain as shown by higher area under curve (AUC) with $p < 0.05$) compared to water mice. (B'') From week 6 onwards (as represented by the dotted line in B), there is an even larger difference between the AUC of sucrose and water mice. Data are presented as mean ±S.E.M; n = 4 mice/group.

4.2 Long term sucrose consumption does not affect SVZ proliferation and neuroblast populations.

Cognitive and memory deficits and a reduction of hippocampal neurogenesis have been reported previously by our lab (Beecher, Alvarez Cooper, et al., 2021).

Therefore, I sought to assess the effects of long-term sucrose consumption on the SVZ neurogenic niche, the location where neuroblasts are born and migrate in chains along the rostral migratory stream to the OB and integrate into the existing circuitry as interneurons.

Mice chronically consuming a high-sucrose diet did not show any change in the overall density of SVZ proliferating cells labelled by EdU (during weeks 10-12) (Figure 11C; $p = 0.4204$, t test) and Ki67 which labelled proliferative cells within the 48 hours prior to harvesting (Figure 11D; $p = 0.1148$, t test). There was also no significant change to the general populations of adult stem cells (B1) as shown by Nestin immunolabeling (Figure E; $p = 0.5648$, t test) or neuroblast populations via doublecortin immunolabeling (DCX+) cells (Figure 11F; $p = 0.7612$, t test). The quantification of proliferative stem cells (Nestin+/Ki67+; Figure 11G; $p = 0.7174$, t test) or neuroblast cells shown through (Ki67+/DCX+; Figure 11H; $p = 0.4707$, t test) also did not indicate any significant difference between two groups. All together, these findings indicate that long term sucrose consumption did not have any effect on proliferative cells within the SVZ.

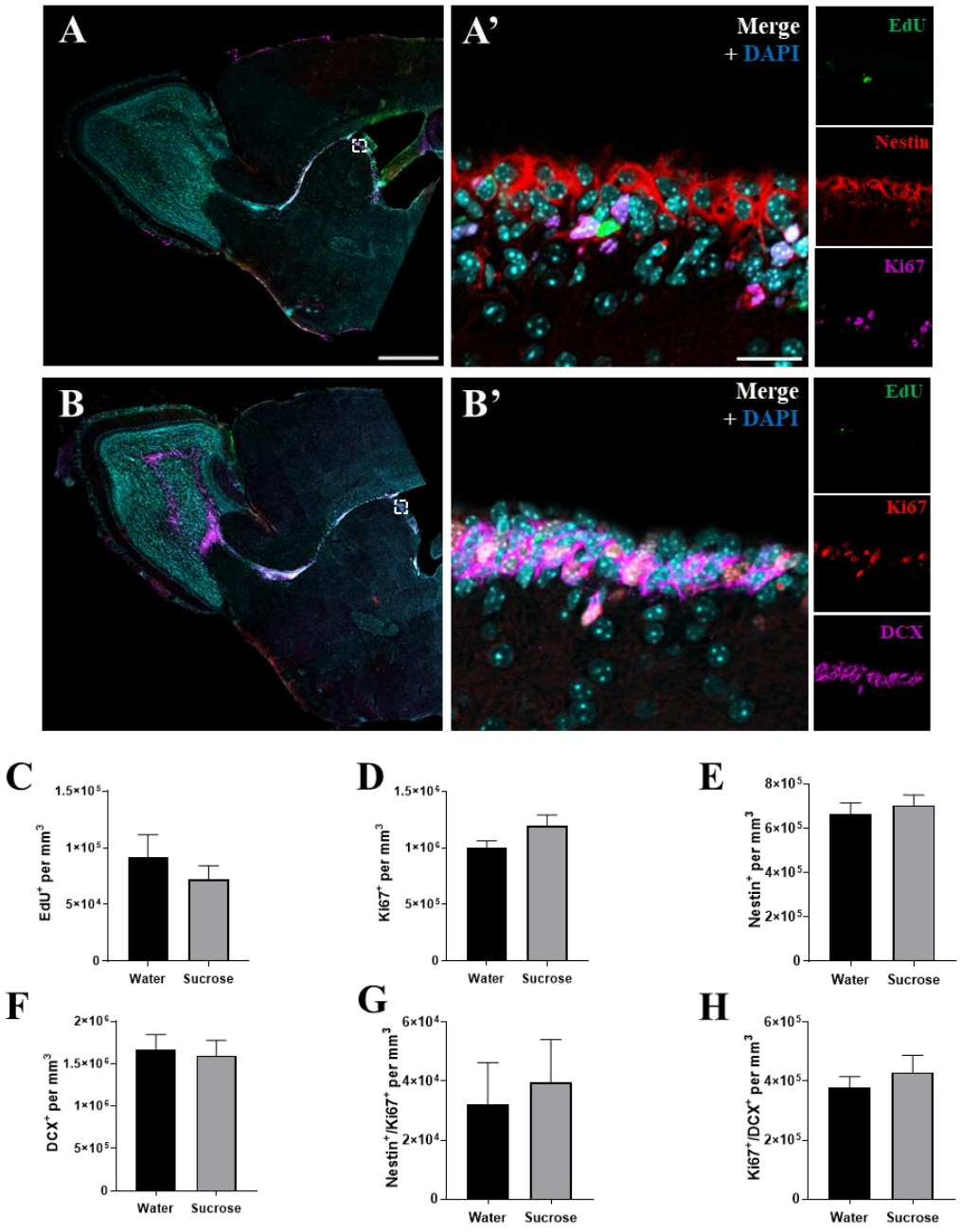

Figure 11: Long term sucrose consumption does not have any effect on SVZ neuroblast populations and proliferating cells

(A) A sagittal section of a mouse brain immunolabelled for Ki67 (red) and DCX (magenta) to highlight the SVZ and RMS. (A') High magnification of the boxed area in the SVZ (A). (B) A low magnification of a brain section immunolabelled for Nestin (red) and Ki67 (magenta) and (B') is a higher magnification of the boxed area. Sucrose consumption did not affect SVZ proliferation as seen through the lack of significant differences in the cell populations of EdU+ (C) and Ki67+ (D). Long-term sucrose consumption did not influence stem cell populations (E) or neuroblast populations (F) in the SVZ. Proliferative neuroblast populations were not affected with sucrose consumption as noted with Ki67+/DCX+ (G) or proliferative B1 stem cells shown through SVZ Nestin+/Ki67+. Scale bar is 500 µm for A, B and 25 µm for A', B'. Data are presented as mean ± S.E.M; n=4 mice/group.

4.3 Long-term sucrose consumption causes neurogenic alterations to the cellular populations in the vertical arm of the RMS.

To assess the effects of sucrose over consumption on RMS, the number of proliferative cells across two representative areas were quantified. The vertical arm, where the SVZ-derived neuroblasts will first congregate and enter the RMS (Figure 12A), the elbow, where it forms an angle (Figure 13A).

The quantifications of proliferative cells within the RMS at the vertical arm did not show any significant difference with neither EdU (Figure 12D; $p = 0.6485$, Two-way ANOVA) nor Ki67 (Figure 12D; $p > 0.9999$, Two-way ANOVA). However, it caused a significant decrease to the population of neuroblasts in the vertical arm (DCX+; Figure 12D; ****$p < 0.0001$, Two-way ANOVA). The reduction in the density of neuroblasts in sucrose consumed animals does not seem to be due to changes to the proliferation of the vertical arm, as there was no difference in the populations of cells double positive for neuronal (Doublecortin: DCX) and proliferative markers (Figure 12D; EdU+/DCX+, $p > 0.9999$, Two-way ANOVA. Ki67+/DCX+, $p > 0.9999$, Two-way ANOVA). To cover a larger area, the number of Edu + cells within 0 – 50 µm distance from either side of the vertical arm were quantified; there were no significant change in number of EdU+ (EdU+; Figure 12E, $p > 0.9999$, Two-Way ANOVA), and Ki67+ cells upon sucrose consumption (Figure 12E, $p = 0.0553$) in this region.

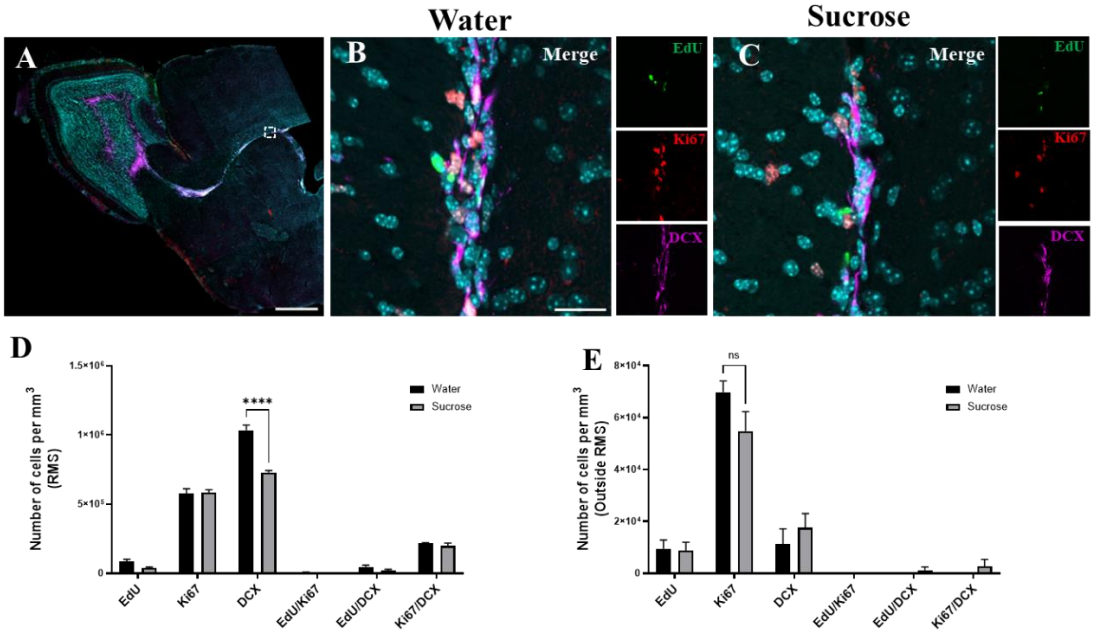

Figure 12: Long-term sucrose consumption causes neurogenic alterations to the cellular populations in the vertical arm of RMS (both within the RMS and the distance area).

(A) Low magnification of a sagittal section of a mouse brain immunolabelled for Ki67 (red) and DCX (magenta) to highlight the SVZ and RMS. A dotted square over the vertical arm of the RMS shows where the higher magnification images (B-C) have been taken from. (D-E) The graphs show the changes in cell populations of EdU+, Ki67+ and DCX+ cells both within the RMS (D) and the area 0 – 50 µm outside of the RMS (E). n = 3 mice per group. *p < 0.05; ****p < 0.0001. Scale bar for A indicates 500 µm and 25 µm for B - C µm. Data are presented as mean ± S.E.M; n=3 mice/group.

4.4 Long-term sucrose consumption does not affect the populations of neuroblasts or proliferative cells of the elbow of the RMS.

Next, the number of proliferative cells of the elbow of the RMS were quantified. The results demonstrated no significant changes to the cell proliferation of the elbow between two groups (Figure 13D; EdU+, $p > 0.9999$. Ki67, $p > 0.8400$, Two-way ANOVA). The DCX immunolabeling of the elbow of the RMS did not show any significant changes between groups (Figure 13D; DCX+; $p > 0.9999$, Two-way ANOVA), and there was no changes to the populations of proliferative neuroblasts in the elbow (Figure 13D; Ki67+/DCX+, $p = 0.9803$, Two-way ANOVA).

Sucrose consumption caused a significant reduction in proliferative cells found around the elbow indicated by Ki67 + cells (Figure 13E, ***p = 0.0001). However, there were no differences in the neuroblast populations (DCX+; Figure 13E, p =

0.1682), and proliferative neuroblasts around the elbow of RMS (Ki67+/DCX+; Figure 13E, p = 0.9999).

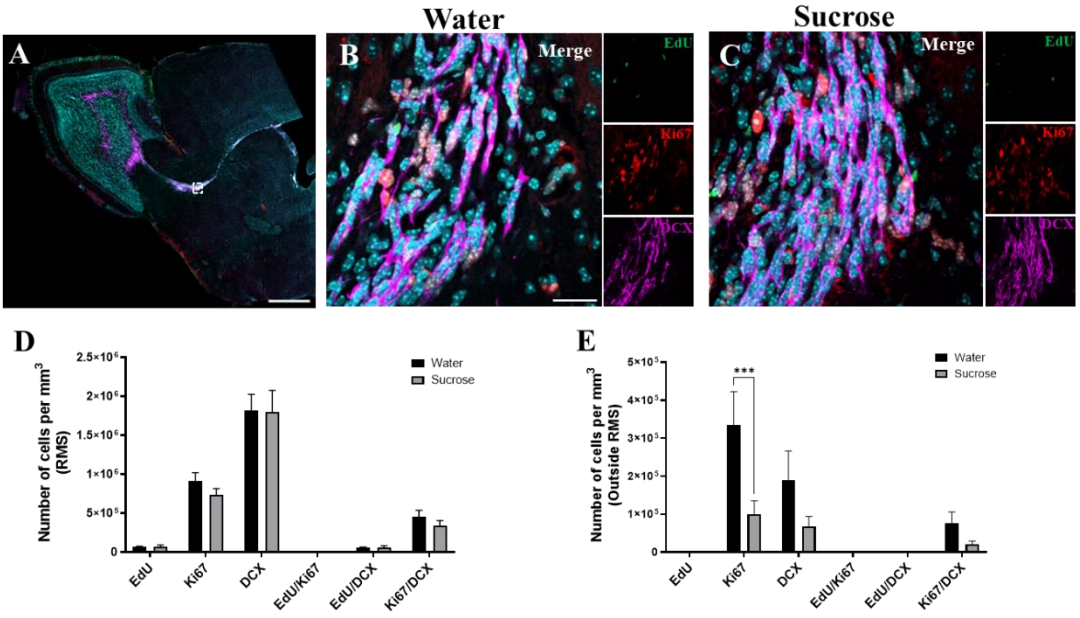

Figure 13: Long-term sucrose consumption does not affect the cellular populations of the elbow of the RMS, however it reduced the populations of proliferative cells around the elbow of the RMS.

(A-C) Immunohistochemical labelling of mouse brains, immunolabelled for Ki67 (red) and DCX (magenta). (A) Low magnification of a sagittal section of a mouse brain immunolabelled for Ki67 and DCX to highlight the SVZ and RMS. A dotted square is placed over the elbow of the RMS to show where the higher magnification images (B-C) were taken. (D-E) The graphs show the changes in cell populations of EdU+, Ki67+ and DCX+ cells both within the RMS (D) and the area 0 – 50 µm outside of the RMS (E). n = 4 animals per group. ***p = 0.0001. The scale bar for A indicates 500 µm and 25 µm for B-C. Data are presented as mean ± S.E.M.

4.5 Long-term sucrose consumption increased the number of calretinin^{+} juxtaglomerular cells.

One of the primary roles of SVZ neurogenesis is to form neuroblasts which will travel through the RMS, arrive to the OB and differentiate into juxtaglomerular interneurons or granule interneurons. Here, I assess if the fate of the cells produced/migrated from SVZ to the OB is affected by sucrose over consumption through quantifying the populations of calbindin+ (CB), calretinin + (CR) and tyrosine hydroxylase+ (TH) interneurons. To which, it was identified that long-term sucrose consumption caused an increase in the number of CB+ juxtaglomerular interneurons (Figure 14C'; *p = 0.0106, t-test). There were no detected changes to the populations of juxtaglomerular CR+ (Figure 14C'''; p = 0.1989) or TH+ interneurons (Figure 16B'; p = 0.9830). The number of CR+ neurons in the granular layer of the olfactory bulb were quantified, and no significant differences between groups was found (Figure 14D; p = 0.4202). The proliferative population of the following neurons did not show any significant changes (CB+/EdU+, Figure 14C'', p = 0.9906; CR+/EdU+, Figure 14C'''', p = 0.2718; TH+/EdU+, Figure 15B'', p = 0.8039). Sucrose consumption also did not affect granular CR+ proliferative cells either (CR+/EdU+; Figure 14C''''; p = 0.4202).

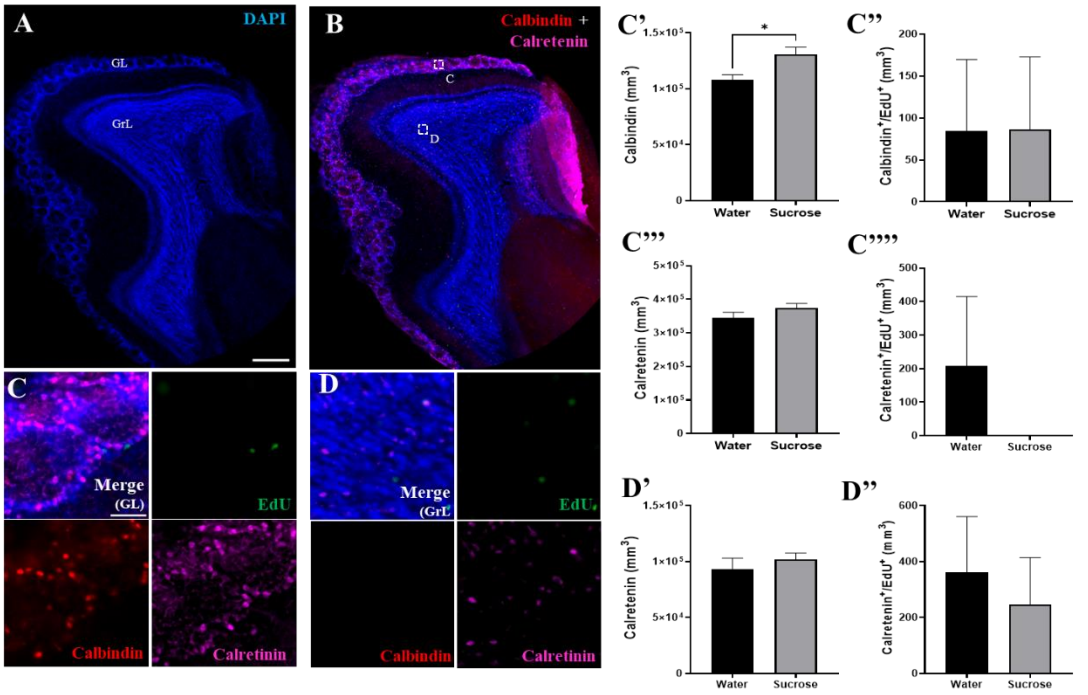

Figure 14: Long-term sucrose consumption increased the population of calbindin+ but not calretinin+ interneurons.

(A-D) Sagittal sections of the OB labelled with DAPI, calbindin (red), calretinin (magenta), and EdU (green) indicating the glomerular layer (GL) and the granular layer (GrL) of the OB. Higher magnification of the boxed areas in the GL and GrL are shown in (C) and (D) respectively. (C-C'''') show juxtaglomerular neurons quantifications. (C') Long term sucrose consumption increased the number of calbindin+ juxtaglomerular cells; however, there was no change to the number of proliferative calbindin+ cells (C''). It also did not affect calretinin+ juxtagomerular populations, nor does it affect calretinin cells proliferation (C''', C''''). (D) Higher magnification images of the GrL. Sucrose consumption did not affect granular calretinin+ populations (D') nor the proliferation of calretinin+ granule cells (D''). Data are presented as mean ± SEM; n = 4 mice per group. *p < 0.05. Scale bar is 300 µm for A and 50 µm for B-C.

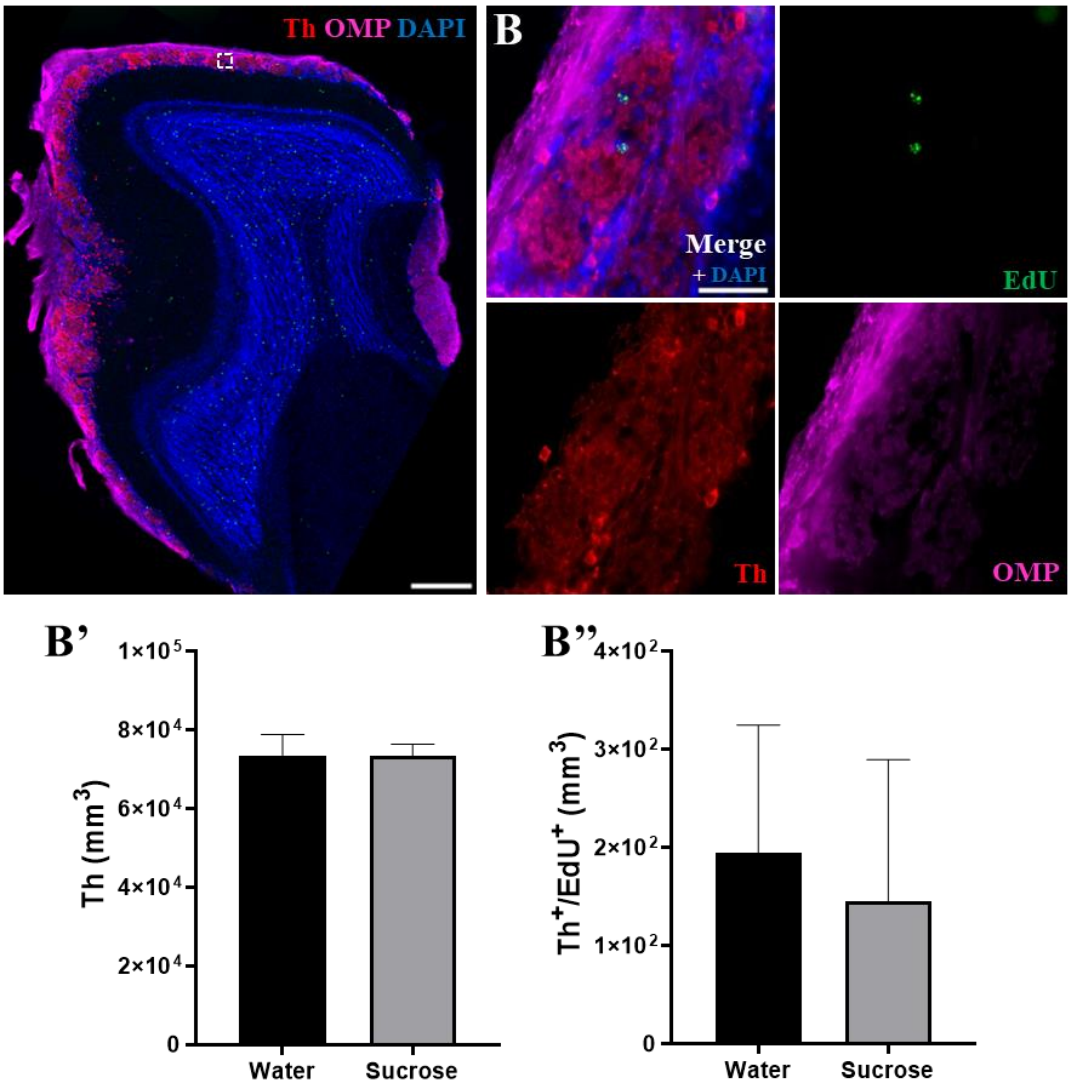

Figure 15: Long-term sucrose consumption did not affect populations of tyrosine hydroxylase juxtaglomerular cells.

(A-B) a sagittal section of the OB labelled with DAPI, tyrosine hydroxylase (TH; red), olfactory marker protein (OMP; magenta) and EdU (green). Higher magnification of the boxed area in the GL is shown in (B). (B'-B'') Long term sucrose consumption did not affect the number of TH+ juxtaglomerular cells, and their proliferative populations. Scale bar is 300 µm for A and 50 µm for B.

4.6 Sucrose consumption affected the astrocytes of the OB but not the microglia.

Next, we assessed whether long term sucrose consumption has any effects on the glial cells of the OB. Astrocytes and microglia have numerous supportive functions in OB interneuron neurogenesis (Martončíková et al., 2021; Meller et al., 2023).

First, I measured the volume of the astrocytes and and total coverage area of the GL layer of the OB. The results showed that sucrose consumption did not have any effect on the mean astrocyte volume (Figure 16D; $p = 0.8712$, t-test), the proportion of astrocytic coverage (Figure 16E, $p = 0.8642$), the number of reconstructed astrocytes in the GL tissue (Figure 16F, $p = 0.7252$), the mean GFAP fluorescence per astrocyte (Figure 16G, $p = 0.8279$) or the normalised mean intensity (Figure 16H, $p = 0.8054$).

However, sucrose did affect the astrocytes of the GrL of the OB. Sucrose consumption caused a significant reduction in the average volume of astrocytes (Figure 16K, ****$p < 0.0001$), the proportion of astrocyte coverage was also reduced in the GrL (Figure 16L, ****$p < 0.0001$). However, there was no affect on the number of astrocytes (Figure 16M, $p = 0.7155$). Sucrose consumption also caused a reduction in the mean GFAP fluorescence intensity per astrocyte (Figure 16N, **$p = 0.0033$) in the GrL. However, when normalised against coverage, sucrose consumption was found to increase the mean fluorescence (Figure 16O, **$p = 0.0021$).

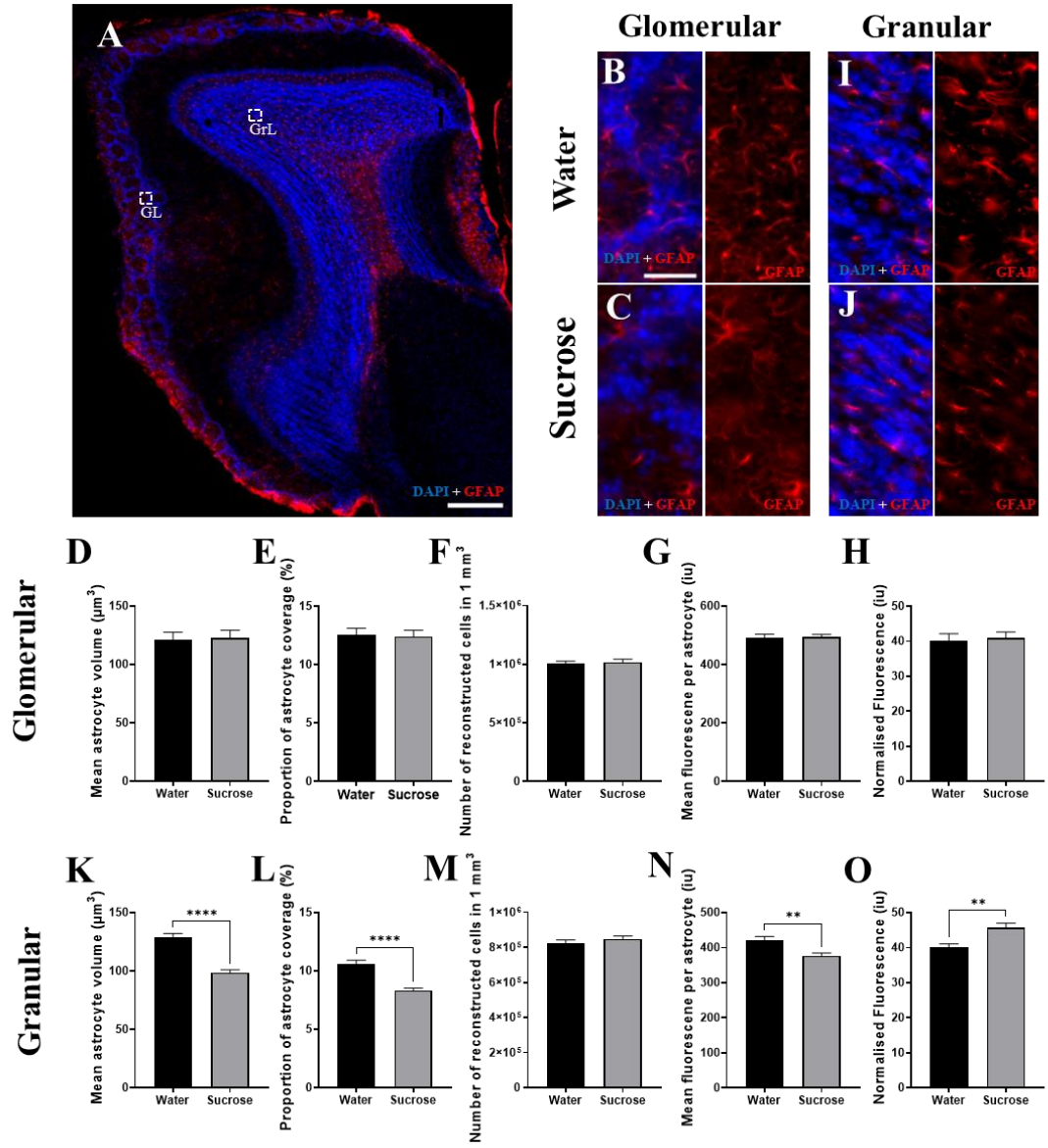

Figure 16: The sucrose consumption reduced astrocytic coverage area in the granular layer but not the glomerular layer.

(A) A sagittal section of the OB labelled with DAPI and glial fibrillary astrocytic protein (GFAP; red). The dashed square in the glomerular layer (GL) represents where the higher magnification images in (B) and (C) were taken. The dashed square in the granule layer (GrL) represents where the higher magnification images in (I) and (J) were taken. (B-H) represent the astrocytes of the GL. (D-H) The effect of sucrose consumption on the volumetric characteristics (D-E), populations (F) and fluorescent properties of astrocytes in the GL (G-H). (I-J) Representative images of astrocytes in the GrL of the OB. (K-O) Graphs indicate quantifications of astrocytes of the GrL. The effect of sucrose consumption on the volumetric characteristics (K-L), populations (M) and fluorescent properties (N-O) of astrocytes in the GrL(M-O). Data are presented as mean ± S.E.M; n=4 mice/group. **p < 0.01; ****p < 0.0001. Scale bar indicates 300 µm for A and 50 µm for B, C, I, J.

Next, the volume of the microglia and total coverage area of microglial processes of the GL layer of the OB were measured. These results indicate that sugar consumption did not significantly affect the mean microglial volume (Figure 17D, $p = 0.1359$, t-test), the proportion of microglia coverage (Figure 17E, $p = 0.9207$), the number of microglia (Figure 17F, $p = 0.2743$), the mean fluorescence per microglia (Figure 17G, $p = 0.6704$) or the normalised mean TMEM119 intensity (Figure 17H, $p = 0.5256$).

The quantification of the microglia and their processes in the GrL also did not show any significant differences in the mean volume (Figure 17K, $p = 0.5924$, t-test), the proportion of microglia coverage (Figure 17L, $p = 0.6563$), the number of microglia (Figure 17M, $p = 0.9914$), the mean TMEM119 fluorescence per microglia (Figure 17N, $p = 0.8599$) or the normalised mean TMEM119 intensity (Figure 17O, $p = 0.4485$).

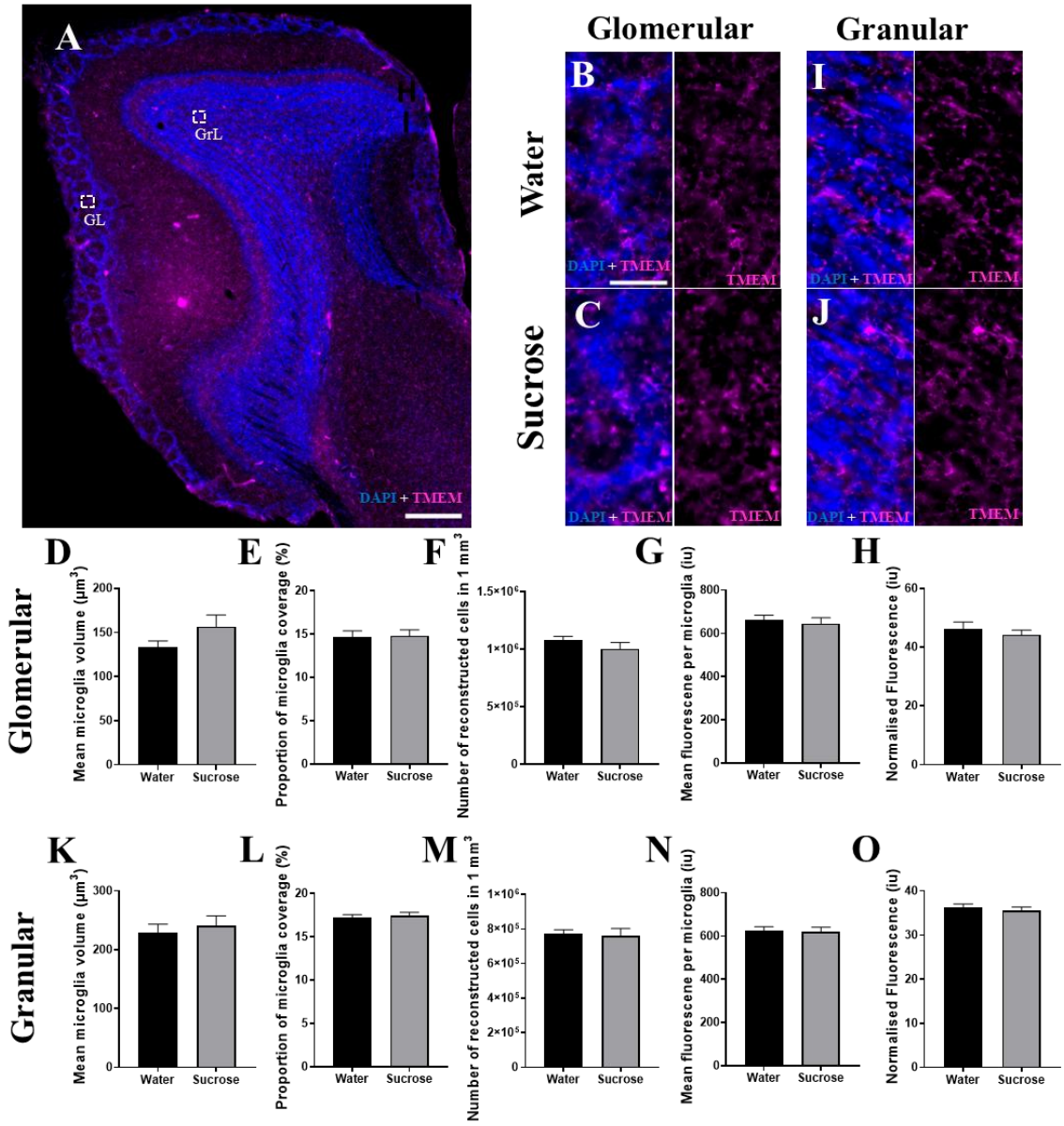

Figure 17: Sucrose consumption did not affect microglia in the glomerular layer or the granular layer of the OB

(A) a sagittal section of the OB labelled with DAPI and transmembrane protein 119 (TMEM119; magenta). The dashed square in the glomerular layer (GL) represents where the higher magnification images (B) and (C) were taken. The dashed square in the granule layer (GrL) represents where the higher magnification images (I) and (J) were taken. Representative images of astrocytes in the GL of the OB of a control animal (B) and a sucrose animal (C). (D-H) Sucrose consumption does not affect the volumetric characteristics (D-E), populations (F) or fluorescent properties of astrocytes in the GL (G-H). Representative images of astrocytes in the GrL of the OB of a control animal (I) and a sucrose animal (J). Sucrose consumption does not affect the volumetric characteristics (K-L), populations (M) or fluorescent properties of astrocytes in the GrL (N-O). Data are presented as mean ± S.E.M; control: n=3; treatment: n=4. Scale bar indicates 300 µm for A and 50 µm for B, C, I, J.

4.7 Sucrose consumption had no significant effect on glial cells populations and proliferation in the OB.

First, the number of general proliferative cells (EdU+) in the GL and GrL of the OB were quantified to investigate whether sucrose consumption affect cell proliferation changes. The results show no difference in the number of general proliferative cells in the GL was not significant (EdU; Figure 18A', p = 0.0702, t-test) and the GrL layers of the OB in sucrose drinking group compared to control (Figure 18A'', p = 0.4397). In addition , there was no significant difference in the number of proliferative astrocytes (GFAP+/EdU+; Figure 18B', p = 0.8891) or proliferative microglia (TMEM+/EdU+; Figure 18C', p = 0.3225) in the GrL layer of the OB.

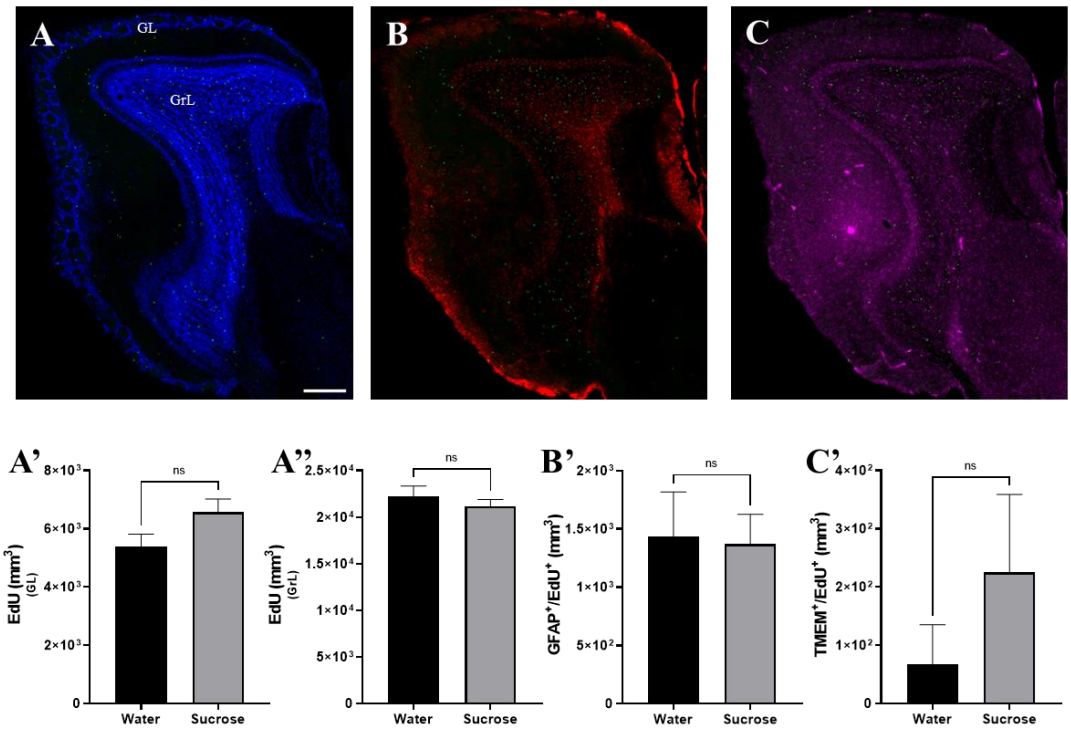

Figure 18: Long-term sucrose consumption did not cause any significant changes to overall OB proliferation and glial cell proliferation

(A) a lower magnification of an OB labelled with DAPI and EdU. The populations of EdU+ cells in the GL (A') and in the GrL (A'') of the OB. (B-B') Sucrose did not significantly affect the density of proliferative astrocytes in the GrL (B'). Similarly, there was no change to the density of proliferative microglia of the GrL (C'). Data are presented as mean ± S.E.M; control: n=4 animals/group. Scale bar for A-C indicates 300 µm.

4.8 Sucrose consumption affected the astrocytes of the SVZ and RMS but not the microglia.

Afterwards, the effect of long-term sucrose consumption on the glial cells of the SVZ and RMS was studied.

The results show that sucrose consumption significantly reduced the mean astrocyte volume (Figure 19D, **p = 0.0040, t-test) and the proportion of astrocyte coverage in the SVZ (Figure 19E, *p = 0.0265). However, there was no difference in the number of reconstructed astrocytes (Figure 19F, p = 0.5459), GFAP fluorescence intensity per astrocyte (Figure 19G, p = 0.0728) or the normalised GFAP fluorescence (Figure 19H, *p = 0.2947) between two groups.

In the RMS, sucrose consumption did not significantly affect the mean astrocyte volume (Figure 219K, p = 0.0727, t-test), and the number of astrocytes (Figure 19M, p = 0.1500). However, the astrocytic coverage of the RMS significantly reduced (Figure 19L, *p = 0.0189). The fluorescent intensity of the RMS astrocytes (per astrocyte) significantly reduced in the sucrose drinking mice (Figure 19N, **p = 0.0062), although there was no change to normalised fluorescence of astrocytes (Figure 19O, p = 0.2995).

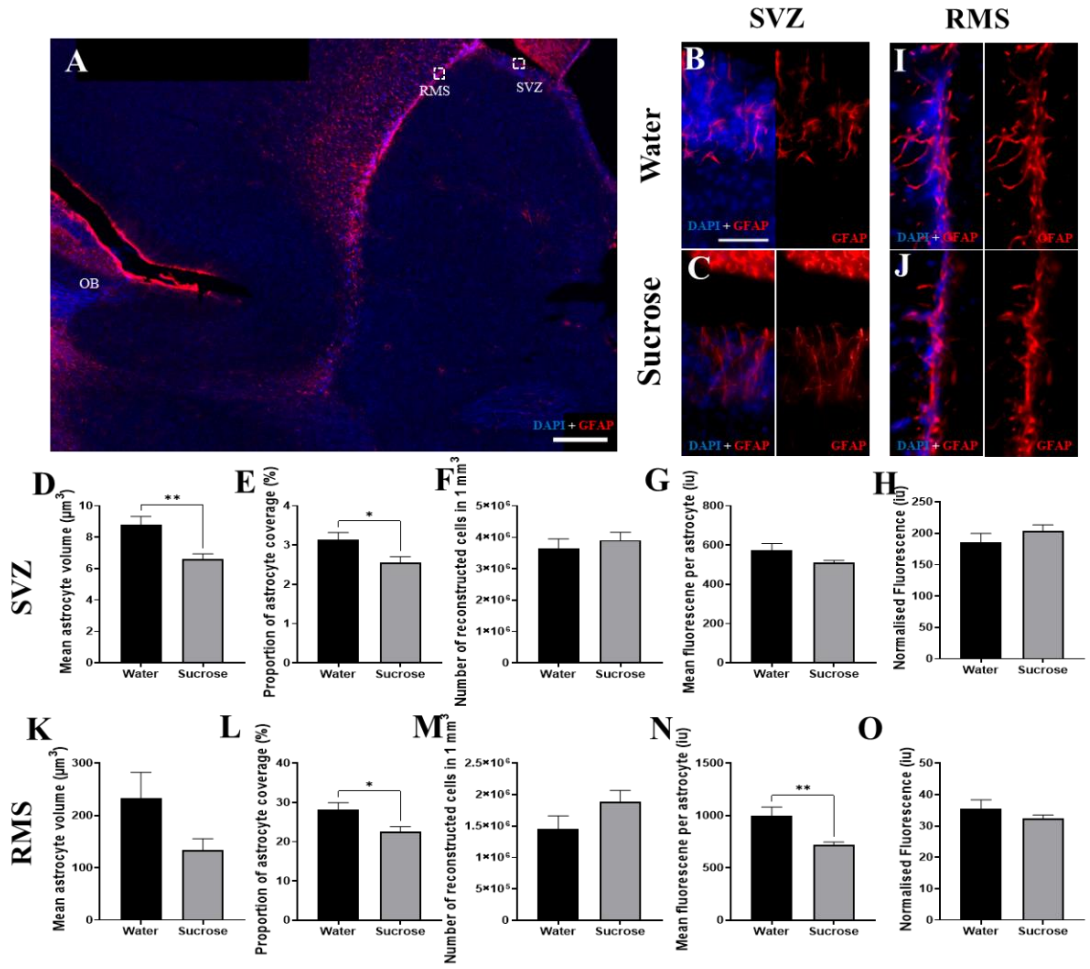

Figure 19: Sucrose consumption affected the astrocytes of the SVZ and RMS

(A) a sagittal section of the OB labelled with DAPI and glial fibrillary astrocytic protein (GFAP; red). The dashed square in the subventricular zone (SVZ) represents where the higher magnification images (B-C) were taken. The dashed square in the rostral migratory stream (RMS) represents where the higher magnification images (I-J) were taken. The effect of sucrose consumption on astrocyte volume (D) and coverage area (E), populations (F) and fluorescent properties (G-H) in the SVZ were presented. Representative images of astrocytes in the RMS of a control animal (H) and a sucrose animal (I). The effect of sucrose consumption on the volumetric characteristics of astrocytes (K-L), populations (M) and fluorescent properties (N-O) in the RMS are demonstrated. Data are presented as mean ± S.E.M; n=4 mice/group. *$p < 0.05$; **$p < 0.01$. Scale bar indicates 300 µm for A and 50 µm for B, C, I, J.

Next, the number of microglia in the SVZ and RMS was quantified. The results indicated that sucrose consumption did not induce a significant change in the mean microglial volume (Figure 20D, $p = 0.6662$, t-test), the proportion of microglial coverage (Figure 20E, $p = 0.1783$), the number of reconstructed microglia (Figure 20F, $p = 0.2894$), the mean fluorescence per microglia (Figure 20G, $p = 0.9341$) or the normalised mean intensity (Figure 20H, $p = 0.1259$) in the SVZ. Sucrose consumption also did not induce any significant differences to the mean microglial volume (Figure

20K, p = 0.4057), the proportion of microglia coverage (Figure 20L, p = 0.2528), the number of reconstructed microglia in tissue (Figure 20M, p = 0.7848), the mean fluorescence per microglia (Figure 20N, p = 0.4778) or the normalised mean intensity (Figure 20O, p = 0.2143) in the RMS. These results show the microglia of these regions were not affected significantly by sucrose consumption.

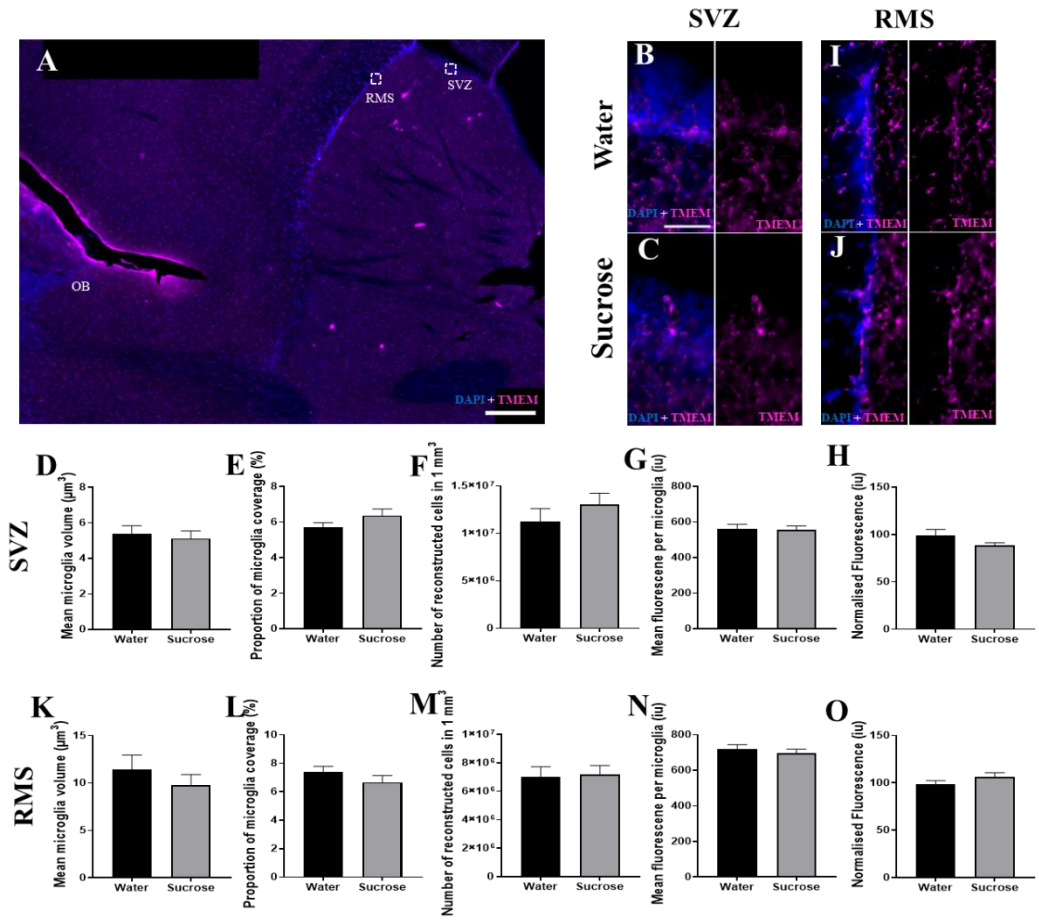

Figure 20: Sucrose consumption did not affect microglia in the SVZ or the RMS

(A) a sagittal section of a mouse brain labelled with DAPI and transmembrane protein 119 (TMEM119; magenta). The dashed square in the subventricular zone (SVZ) represents where the higher magnification images (B-C) were taken. The dashed square in the rostral migratory stream (RMS) represents where the higher magnification images (I-J) were taken. The effect of sucrose consumption on the volumetric characteristics (D-E), populations (F) and fluorescent properties (G-H) of microglia in the SVZ are presented. The effect of sucrose consumption on the volumetric characteristics (K-L), populations (M) and fluorescent properties (N-O) of microglia in the RMS are illustrated. Data are presented as mean ± S.E.M; control: n=3; treatment: n=4. Scale bar indicates 300 µm for A and 50 µm for B, C, I, J.

Chapter 5: Discussion

The relationship between sugar consumption and obesity has been well documented (Bentley et al., 2020). With high body mass being one of the major contributors to Australia's total disease burden (Australian Institute of Health and Welfare, 2016), it is important for researchers to understand the burden that a high-caloric diet has on the body and brain. Indeed, obesity is known to affect different types of memory, including episodic memory and obese children are known to have deficits in memory among other cognitive functions (Loprinzi & Frith, 2018; Meo et al., 2019; Wu et al., 2017). Using a well-established animal model, we have been able to identify that sucrose consumption caused memory deficits with reduced hippocampal neurogenesis (Beecher, Alvarez Cooper, et al., 2021). Obesogenic diets have been known to alter glial cell behaviour in appetite-related areas such as the hypothalamus, causing increased hunger (Valdearcos et al., 2017). Considering these examples in which diet impairs health outcomes and altered both neurogenic and appetite-related areas of the brain, I wanted to understand if sucrose consumption affects other neurogenic regions of the brain related to appetite, such as the SVZ, RMS and OB. The SVZ is a neurogenic niche in the brain which persists postnatally. It creates neuroblasts which will travel via the RMS and into the OB where they will reach their target destination and differentiate into olfactory interneurons. The OB is important for appetite regulation (Palouzier-Paulignan et al., 2012), and more specifically, the OB interneurons have been associated with odour detection, judgement of odour information, and long-term odour memory (Lazarini et al., 2009; Sakamoto et al., 2014; Wu et al., 2020). I initially examined the effect of long-term sucrose consumption on SVZ, RMS and OB neurogenesis. Then I assessed the effects

of high-sucrose diet on OB interneurons. Lastly, I studied the effect of sucrose consumption on the glial cells of these regions.

5.1 The effect of sucrose consumption on the SVZ and RMS neurogenesis

The SVZ and the RMS are brain structures which initiate OB interneuron neurogenesis; therefore, they are crucial areas in the investigation of the effect of sucrose consumption on forebrain neurogenesis.

5.1.1 Sucrose consumption did not affect the SVZ neurogenesis.

The results showed no significant difference in NSCs, called type B1 cells ($Nestin^+$ cells), neuroblast populations (DCX^+ cells) and proliferative cell populations ($Ki67^+$ cells and EdU^+ cells). There were also no changes in the stem cell proliferation ($Ki67^+/Nestin^+$ cells) or neuroblast proliferation ($Ki67^+/DCX^+$ cells and EdU^+/DCX^+ cells). These results differ from literature whereby the introduction of an injury vehicle caused a burst of proliferation in the SVZ (Franco et al., 2014). Similarly, but more specific to carbohydrate consumption, an increase of glucose intake was also found to increase SVZ and hippocampal neurogenesis (Lang et al., 2009). The differences in experimental designs may have contributed to these variations, considering they investigated the effect of hyperglycaemia induced by high glucose-consumption in a type 2 diabetes rat model, which is very different from our animal model (Beecher, Alvarez Cooper, et al., 2021). Fructose is known to significantly reduce hippocampal neurogenesis in rats (Fierros-Campuzano et al., 2020; van der Borght et al., 2011) and mice (Cisternas et al., 2015). As sucrose is a disaccharide made of fructose and glucose, there is a possibility that these two saccharides induce different effects when they are used individually or combined. It is worth noting that recently our lab found that long-term sucrose consumption reduced hippocampal neurogenesis (Beecher, Alvarez Cooper, et al., 2021). While the current investigation did not see any changes

to SVZ proliferation and neurogenic populations, more research needs to be undertaken to understand whether sucrose consumption effects cell viability of the SVZ region.

5.1.2 RMS

The number of proliferative cells and neuroblasts of two different areas of the RMS were quantified to assess the effect of sucrose consumption on the RMS. The two areas were at the vertical arm and the elbow.

Vertical arm – These data demonstrate that long-term sucrose consumption caused a significant reduction of neuroblasts (DCX^+) in the vertical arm of the RMS. This is quite interesting considering the vertical arm is the most proximal portion of the RMS, the location where the SVZ-derived neuroblasts first enter the RMS from the SVZ and sucrose consumption did not change general proliferative cell populations of SVZ neuroblasts or proliferating neuroblasts. This is a finding consistent in literature whereby upon the admission of an injury vehicle, populations in the SVZ and the RMS did not directly corelate (Franco et al., 2014). It was found that the injury vehicle caused a burst of proliferation in the SVZ, however there was no changes to the populations of neuroblasts traveling in the RMS. These results showed that SVZ populations do not directly correlate with RMS populations, and that RMS populations may reduce while SVZ populations remain high (Franco et al., 2014). In the current study, there was a reduction of neuroblasts in the vertical arm; however, there were no changes to SVZ neurogenesis. To explain this phenomenon, there are a few theories: (1) that sucrose consumption affects neuroblast migration from the SVZ to the RMS, (2) that there is an increased rate of neuroblast migration out of the vertical arm of the RMS or (3) that sucrose consumption might affect the viability of SVZ-derived neuroblasts. To theorise that the migration of neuroblasts out of the SVZ (1) is

probably unlikely considering that that would likely result in an accumulation of neuroblasts in the SVZ, which was not observed here. To theorise that there is increased migration out of the vertical arm of the RMS (2) is also a less likely primary contributor to this phenomenon. It is normal for small populations of proliferative cells and neuroblasts to exit the RMS and migrate to different structures, including the corpus collosum, the striatum or the olfactory tubercle (Bédard et al., 2002). Under pathological conditions the number of cells leaving the RMS can be increased (Angelidis et al., 2018; Herzine et al., 2016). For this reason, the cells that were within the structures neighbouring the RMS (0-50 µm outside of either side of the RMS) were also quantified. These structures include the corpus collosum and the striatum. In which case, there were no significant differences to the number of cells migrating out of the RMS. Therefore, it is likely that sucrose consumption disrupts the viability of SVZ-derived neuroblasts, which could be studied in future experiments.

Elbow – Next, the effect of sucrose consumption on the elbow of the RMS. It was found that sucrose consumption did not change any of the cellular populations within the RMS at the level of the elbow. There were no detectable changes to the populations of proliferative cells, neuroblasts or proliferating neuroblasts. This is striking considering sucrose consumption caused a significant reduction to the population of neuroblasts in the vertical arm. These results occur alongside a significant decrease in the number of $Ki67^+$ cells migrating out of the elbow. There are two main possibilities that could have contributed to this finding, one is experimental and the other is anatomical. The experimental reason is associated with the fact that this study was only conducted at one time point. For future experimentation, investigating more timepoints would allow for a more complete view of the migration and survival of neurogenic cells from the SVZ, through the RMS and to the OB.

At the level of the elbow, there is another lesser known minor ‘offshoot’ of the RMS called the posterior limb, or the ventrocaudal migratory stream (VMS; Bédard et al., 2002; De Marchis et al., 2004; Inta et al., 2010). The VMS extends caudally from the elbow of the RMS and sends a small collection of cells to the olfactory tubercle (De Marchis et al., 2004). The results showed that at the level of the elbow, sucrose consumption caused a significant reduction in the number of Ki67 cells outside of the RMS. In total, it is possible that with a significant reduction of neuroblasts at the vertical arm under the conditions of sucrose consumption, the RMS may prioritise intra-RMS cellular populations and reduce the number of cells that are able to migrate out of the RMS to surrounding tissues. The VMS is not a well-known structure, and very little research has been done to assess how changes in diet or environment may affect it. To look further into this theory, future work analysing the VMS and the olfactory tubercle cell populations would be recommended.

Altogether, sucrose consumption did not affect initial proliferation and neuroblast differentiation in the SVZ. There was a significant reduction in the number of neuroblasts in the vertical arm of the RMS. However, this result did not affect the number of neuroblasts in the more distal part of the RMS as there were no significant reductions to the populations of neuroblasts at the elbow of the RMS. These results indicate that the populations of neuroblasts and proliferative cells reaching the OB were no different between groups. This stabilisation of neuroblast populations correlates with a marked reduction in the number of proliferative cells migrating out of the RMS at the elbow suggest the possibility that the RMS may prioritise the intra-RMS neuroblast populations.

5.2 The effect of sucrose consumption on OB interneuron populations.

After investigating the effect of sucrose consumption on SVZ and RMS proliferation and neuroblast populations, I studied the effect of sucrose consumption on the populations of interneurons in the OB; the cells that the SVZ/RMS neuroblasts will differentiate into. The juxtaglomerular interneurons of the OB may be classified by their immunoreactivity to three subtypes of CB^+, CR^+ or TH^+. Meanwhile the interneurons of the GL are primarily CR^+. Each of these interneuron cell types were quantified in sucrose-consuming and control group mice to determine if sucrose consumption effects their populations. It was found that sucrose consumption causes a significant increase in CB^+ juxtaglomerular populations, and no significant changes to the populations of CR^+ and TH^+ juxtaglomerular cells, or granule cells.

The significant increase in CB^+ juxtaglomerular cells upon sucrose consumption was accompanied by no changes in CB^+/EdU^+ cells, indicating that the increase may not be due to an increase in CB^+ proliferation. The reason behind the increase remains unclear considering that sucrose consumption did not cause any significant differences to the number of neuroblasts travelling to the OB. There is a possibility that the CB^+ interneurons may have a higher viability under sucrose consumption due to increased sensory enrichment. The treatment mice had an enhanced olfactory experience with the addition of sucrose in their diet, as opposed to control mice who only received food and water.

The general saying for the body, and indeed also the brain, is “if you don’t use it, you lose it", which is precisely what happens with OB interneuron populations. Nostril occlusion, and thus sensory deprivation, was found to significantly decrease the populations of TH^+ PG cells but not CB^+ or CR^+ cells (Bastien-Dionne et al., 2010). Another study showed that housing animals in an odour enriched environment caused

an increase in TH^+ glomerular cells but not in CB^+ or CR^+ glomerular cells (Bonzano et al., 2014). These results show that changes to the sensory environment can alter the populations of interneurons of the GL. However, an obvious difference between the findings previously stated and the findings of this study is that sucrose consumption had caused no effect on TH^+ juxtaglomerular cells and only increased the number of CB^+ juxtaglomerular cells. Differences in experimental protocol may be the reason of these discrepancies as the nasal occlusion could cause degeneration of the olfactory receptor neurons (Bastien-Dionne et al., 2010) and sucrose consumption was not part of odour enrichment (Bonzano et al., 2014). Duration of the treatment time could be another factor as the interneuron subtypes have a different lifespan (Kohwi et al., 2007). TH^+ cells are regarded as having a faster turnover rate than CB^+ and CR^+ (Kohwi et al., 2007). Also, these studies were specifically looking at the effect of olfactory stimuli on OB interneuron populations; however, the current study introduces an enhanced in olfactory stimuli through a change in diet, the consumption of a sucrose drink. The addition of the changes to blood glucose/fructose levels is an obvious change, specifically when sucrose consumption is known to be associated with addictive pathways in the brain (Jacques et al., 2019). The OB receives input from serotonergic neurons from the medial and dorsal raphe (Capsoni et al., 2021). Therefore, sucrose consumption turning to an appetite addiction may contribute to the changes of interneuron populations.

5.3 Effect of sucrose consumption on glial cells of the OB, RMS and SVZ

Glial cells are crucial for maintaining normal brain homeostasis. Microglia and astrocytes both have regulatory roles for maintaining normal OB, RMS and SVZ functions, both of which are likely to change their behaviour to external stimuli. The

behaviour of microglia and astrocytes within the SVZ, RMS and OB were examined to achieve a better understanding of the effect of sucrose consumption.

A range of different glial cell properties were measured, including their volume, cover surface areas, populations, proliferation rate and fluorescent intensity. We quantified these factors in the GL and GrL of the OB, the SVZ and the vertical arm of the RMS.

Sucrose consumption changed the behaviour of GrL astrocytes of the OB. The results showed that sucrose consumption significantly reduced the astrocytic volume and astrocyte coverage in the GrL. The reduced coverage accompanied by the same number of reconstructed astrocytes shows that the reduced coverage is attributed to the reduced astrocyte volume and not to changes in cell populations.

Sucrose consumption was also shown to reduce the GFAP florescent intensity of individual astrocytes, but when normalised against coverage, the GFAP fluorescence of the sucrose group was significantly higher than the control group. However, there were no differences in astrocyte populations, volume, coverage, and GFAP fluorescent intensity of the GL of the OB. As of the SVZ, sucrose consumption significantly reduced the mean astrocyte volume, and the proportion of astrocytic coverage. As, there were no changes to the number of reconstructed astrocytes in tissue, it is indicated that the reduced astrocyte coverage is likely attributed to the reduced volume per astrocyte. As of the RMS, sucrose consumption significantly reduced the proportion of astrocyte coverage and the mean fluorescence per astrocyte. There were was also a reduction in astrocytic coverage of the area. Generally, these findings contribute to the growing evidence that astrocytes do not express a ‘uniform’ morphology throughout brain structures instead express a morphology that is region specific (Torres-Platas et al., 2016). In terms of characterising astrocyte behaviour,

there are many documented instances of increases of astrocyte volume through process extension and astrogliosis (J.-M. Li et al., 2015; Torres-Platas et al., 2016). Excessive sugar consumption has been known to induce astrogliosis in other brain structures (J.-M. Li et al., 2015, 2019; Salvadó et al., 2022). However, very little research has been done to assess the effect of sucrose consumption on the SVZ, RMS and OB. This is especially important considering the astrocytes of these areas are very closely associated with newborn neurons and undergo changes in morphology as a result of neuroblast interactions (Martončíková et al., 2021). Neuroblasts are known to repel astrocytic processes and can even make direct contact with blood vessels (Kaneko et al., 2010; Peretto et al., 1999, 2005; Whitman et al., 2009). Blood vessels and astrocytes also have an important role in neuroblast migration, whereby neuroblasts take up the BDNF released by endothelial cells, allowing them to migrate, and astrocytes are then able to upregulate a receptor for BNDF, TrkB, and outcompete the neuroblasts so as to 'collect' the excess BDNF from the extracellular matrix (Snapyan et al., 2009). Altogether, this information could explain the decrease in astrocyte volume with sucrose consumption. The results regarding the effect of sucrose consumption on the RMS lead us to speculate that the RMS may prioritise intra-RMS neuroblast populations. It can be speculated that the lower neuroblast populations at the vertical arm of the RMS may cause the neuroblasts to upregulate their repulsion of astrocytic processes so that the neuroblasts may maintain better contact with the blood vessel scaffold to prioritise neuroblast uptake of BDNF. To explore this, further study covering the relationship between neuroblasts, astrocytes and blood vessels in sucrose drinking animals is recommended. It would be also beneficial to determine if sucrose consumption changes the expression of TrkB receptor on astrocytes.

The microglia of the OB (GL and GrL) did not undergo any significant changes under sucrose consumption. Similarly, sucrose consumption did not induce any significant changes in the microglia of the SVZ or RMS. Obesogenic diets such as high-fat diets are known to increase microglial populations and alter their morphology to be more pro-inflammatory within the hypothalamus (Chen et al., 2021; Dorfman & Thaler, 2015). High fat and high sugar diets have been found to increase hypothalamic microglial response in male mice (Daly et al., 2022). Although, it is difficult to apply this diet framework on the experiments detailed in this report as it includes high fat in this obesogenic diet, which has already been found to illicit changes to microglial behaviour. However very little research has been done to study the effect of sucrose consumption on microglial activity on the SVZ, RMS and OB. These results are the first to show that microglia may not be affected by sucrose in the areas of the SVZ, RMS and OB. However further studies covering larger cohort of animals and different time points with sucrose over consumptions is recommended.

Chapter 6: Conclusions

6.1 Conclusion

This investigation provided a unique insight into the effect of sucrose consumption on SVZ and RMS neurogenesis along with OB interneuron populations. Populations of SVZ neurogenic cells were not affected by sucrose consumption. However, neuroblast populations in the vertical arm of the RMS were significantly reduced in sucrose animals, a reduction which was attenuated as of the elbow whereby neuroblast populations were the same between sucrose and water animals. This study found that sucrose consumption causes significant increase in calbindin^{+} juxtaglomerular cells. In addition, astrocyte volume, GFAP fluorescent intensity labelling and populations were often reduced with sucrose consumption.

6.2 Limitations

There are some limitations regarding the sex, age and strain of mice used in this investigation. Limiting the study group to only using the male sex gives rise to the possibility of missing the effect of sucrose consumption on female mice. Adolescent sucrose consumption is far higher than that of adults, prompting us to commence sucrose consumption in mice during their adolescence. It is worth noting that previous studies have found less of an impact of sucrose consumption after adolescence and have recommended studying the effect of sucrose over longer time periods (Kendig, 2014). Using different mouse strains might also be beneficial as it is known that sucrose consumption can have varied effects between different strains of mice (Kendig et al., 2014).

Using a slide scanner to image the GFAP and TMEM stains is a limitation regarding the quality of data generated from the Imaris software. While the thresholds

were altered to minimise the amount of background, using a slide scanner means that there is some fluorescence artifact that will be derived from throughout the z-stack. This will mean that the volume measurement of an object would be dependent on the object's fluorescence. To rectify this, it is worth noting that the control and treatment group brain sections were all immunolabelled concurrently and imaged under the same settings to minimise bias.

Another limitation was through classifying all $GFAP^+$ objects in the SVZ as astrocytes. Adult stem cells at certain stages may also express GFAP. Indicating the possibility that some of the "astrocyte" objects noted by Imaris may be a B1 cell at some sort of stage of division instead of an astrocyte.

The group size of n = 4 was another limitation in this study. As mentioned in section 3.2, the original G*power analysis proposed that a minimum of n = 8 would be optimal to derive data from this study. However, the group sizes were reduced to n = 4 as this was a pilot study. This pilot investigation was promising, as it showed that sucrose consumption does affect SVZ neurogenesis, OB interneuron populations and astrocyte populations and morphology. It is worth noting that while all data was derived from n = 3 or n = 4, statistical test showed that the data was normally distributed, confirming the viability of the data. In the future experiment, additional animals (n= 5) to repeat the experiments will be necessary to complete the study.

6.3 Future directions

The interaction between astrocytes, blood vessels and neuroblasts of the SVZ, RMS and OB need to be further examined to possibly help clarify the cause of the reduced volume and coverage of astrocytes in these areas. Concurrently, investigating the way in which the RMS can prioritise intra-RMS cell populations is necessary to explain the results gathered. The reduced GFAP expression in astrocytes under sucrose

consumption may have important implications for other diseases (Moody et al., 2017). Techniques such as tissue culture should be considered to examine characteristics of the astrocytes *in vitro* in response to sucrose in culture medium. Considering multiple time points/exposure time will allow us to understand the long-term effects of sucrose consumption on OB interneuron populations in more details.

Bibliography

Abbott, L. C., & Nigussie, F. (2020). Adult neurogenesis in the mammalian dentate gyrus. *Anatomia, Histologia, Embryologia*, *49*(1), 3–16. https://doi.org/10.1111/ahe.12496

Alfonso, J., Penkert, H., Duman, C., Zuccotti, A., & Monyer, H. (2015). Downregulation of Sphingosine 1-Phosphate Receptor 1 Promotes the Switch from Tangential to Radial Migration in the OB. *The Journal of Neuroscience*, *35*(40), 13659–13672. https://doi.org/10.1523/JNEUROSCI.1353-15.2015

Angelidis, A., Račeková, E., Arnoul, P., Závodská, M., Raček, A., & Martončíková, M. (2018). Disrupted migration and proliferation of neuroblasts after postnatal administration of angiogenesis inhibitor. *Brain Research*, *1698*, 121–129. https://doi.org/10.1016/j.brainres.2018.08.010

Anjum, I., Jaffery, S. S., Fayyaz, M., Wajid, A., & Ans, A. H. (2018). Sugar Beverages and Dietary Sodas Impact on Brain Health: A Mini Literature Review. *Cureus*, *10*(6), e2756. https://doi.org/10.7759/cureus.2756

Apovian, C. M. (2016). Obesity: Definition, comorbidities, causes, and burden. *The American Journal of Managed Care*, *22*(7 Suppl), s176-185.

Australian Bureau of Statistics. (2018, December 12). *Overweight and obesity, 2017-18 financial year*. https://www.abs.gov.au/statistics/health/health-conditions-and-risks/overweight-and-obesity/latest-release

Australian Institute of Health and Welfare. (2016). *Australia's health 2016.*

Avena, N. M., Rada, P., & Hoebel, B. G. (2008). Evidence for sugar addiction: Behavioral and neurochemical effects of intermittent, excessive sugar intake. *Neuroscience & Biobehavioral Reviews*, *32*(1), 20–39. https://doi.org/10.1016/j.neubiorev.2007.04.019

Baier, P. C., Weinhold, S. L., Huth, V., Gottwald, B., Ferstl, R., & Hinze-Selch, D. (2008). Olfactory dysfunction in patients with narcolepsy with cataplexy is restored by intranasal Orexin A (Hypocretin-1). *Brain*, *131*(10), 2734–2741. https://doi.org/10.1093/brain/awn193

Bastien-Dionne, P.-O., David, L. S., Parent, A., & Saghatelyan, A. (2010). Role of sensory activity on chemospecific populations of interneurons in the adult olfactory bulb. *Journal of Comparative Neurology*, *518*(10), 1847–1861. https://doi.org/10.1002/cne.22307

Batista-Brito, R., Close, J., Machold, R., & Fishell, G. (2008). The Distinct Temporal Origins of Olfactory Bulb Interneuron Subtypes. *The Journal of Neuroscience*, *28*(15), 3966–3975. https://doi.org/10.1523/JNEUROSCI.5625-07.2008

Bayard, S., Plazzi, G., Poli, F., Serra, L., Ferri, R., & Dauvilliers, Y. (2010). Olfactory dysfunction in narcolepsy with cataplexy. *Sleep Medicine*, *11*(9), 876–881. https://doi.org/10.1016/j.sleep.2010.07.004

Beal, J. A. (2020). World Health Organization Alert on High Level of Sugar in Baby Food. *MCN: The American Journal of Maternal/Child Nursing*, *45*(1), 60. https://doi.org/10.1097/NMC.0000000000000584

Bédard, A., Lévesque, M., Bernier, P. J., & Parent, A. (2002). The rostral migratory stream in adult squirrel monkeys: Contribution of new neurons to the olfactory tubercle and involvement of the antiapoptotic protein Bcl-2. *European Journal of Neuroscience*, *16*(10), 1917–1924. https://doi.org/10.1046/j.1460-9568.2002.02263.x

Beecher, K., Alvarez Cooper, I., Wang, J., Walters, S. B., Chehrehasa, F., Bartlett, S. E., & Belmer, A. (2021). Long-Term Overconsumption of Sugar Starting at

Adolescence Produces Persistent Hyperactivity and Neurocognitive Deficits in Adulthood. *Frontiers in Neuroscience*, *15*, 670430. https://doi.org/10.3389/fnins.2021.670430

Beecher, K., Wang, J., Jacques, A., Chaaya, N., Chehrehasa, F., Belmer, A., & Bartlett, S. E. (2021). Sucrose Consumption Alters Serotonin/Glutamate Co-localisation Within the Prefrontal Cortex and Hippocampus of Mice. *Frontiers in Molecular Neuroscience*, *14*, 678267. https://doi.org/10.3389/fnmol.2021.678267

Beilharz, J. E., Kaakoush, N. O., Maniam, J., & Morris, M. J. (2016). The effect of short-term exposure to energy-matched diets enriched in fat or sugar on memory, gut microbiota and markers of brain inflammation and plasticity. *Brain, Behavior, and Immunity*, *57*, 304–313. https://doi.org/10.1016/j.bbi.2016.07.151

Beilharz, J. E., Maniam, J., & Morris, M. J. (2014). Short exposure to a diet rich in both fat and sugar or sugar alone impairs place, but not object recognition memory in rats. *Brain, Behavior, and Immunity*, *37*, 134–141. https://doi.org/10.1016/j.bbi.2013.11.016

Belmer, A., Patkar, O. L., Lanoue, V., & Bartlett, S. E. (2018). 5-HT1A receptor-dependent modulation of emotional and neurogenic deficits elicited by prolonged consumption of alcohol. *Scientific Reports*, *8*(1), 2099. https://doi.org/10.1038/s41598-018-20504-z

Bentley, R. A., Ruck, D. J., & Fouts, H. N. (2020). U.S. obesity as delayed effect of excess sugar. *Economics and Human Biology*, *36*, 100818. https://doi.org/10.1016/j.ehb.2019.100818

Boldrini, M., Fulmore, C. A., Tartt, A. N., Simeon, L. R., Pavlova, I., Poposka, V., Rosoklija, G. B., Stankov, A., Arango, V., Dwork, A. J., Hen, R., & Mann, J. J. (2018). Human Hippocampal Neurogenesis Persists throughout Aging. *Cell Stem Cell*, *22*(4), 589-599.e5. https://doi.org/10.1016/j.stem.2018.03.015

Bonzano, S., Bovetti, S., Fasolo, A., Peretto, P., & De Marchis, S. (2014). Odour enrichment increases adult-born dopaminergic neurons in the mouse olfactory bulb. *European Journal of Neuroscience*, *40*(10), 3450–3457. https://doi.org/10.1111/ejn.12724

Bortolin, R. C., Vargas, A. R., Gasparotto, J., Chaves, P. R., Schnorr, C. E., Martinello, K. B., Silveira, A. K., Rabelo, T. K., Gelain, D. P., & Moreira, J. C. F. (2018). A new animal diet based on human Western diet is a robust diet-induced obesity model: Comparison to high-fat and cafeteria diets in term of metabolic and gut microbiota disruption. *International Journal of Obesity (2005)*, *42*(3), 525–534. https://doi.org/10.1038/ijo.2017.225

Bovetti, S., Hsieh, Y.-C., Bovolin, P., Perroteau, I., Kazunori, T., & Puche, A. C. (2007). Blood Vessels Form a Scaffold for Neuroblast Migration in the Adult Olfactory Bulb. *The Journal of Neuroscience*, *27*(22), 5976–5980. https://doi.org/10.1523/JNEUROSCI.0678-07.2007

Bozoyan, L., Khlghatyan, J., & Saghatelyan, A. (2012). Astrocytes Control the Development of the Migration-Promoting Vasculature Scaffold in the Postnatal Brain via VEGF Signaling. *The Journal of Neuroscience*, *32*(5), 1687–1704. https://doi.org/10.1523/JNEUROSCI.5531-11.2012

Brambilla, R. (2019). The contribution of astrocytes to the neuroinflammatory response in multiple sclerosis and experimental autoimmune

encephalomyelitis. *Acta Neuropathologica*, *137*(5), 757–783. https://doi.org/10.1007/s00401-019-01980-7

Bray, G. a., Kim, K. k., Wilding, J. p. h., & Federation, on behalf of the W. O. (2017). Obesity: A chronic relapsing progressive disease process. A position statement of the World Obesity Federation. *Obesity Reviews*, *18*(7), 715–723. https://doi.org/10.1111/obr.12551

Brunert, D., & Rothermel, M. (2021). Extrinsic neuromodulation in the rodent olfactory bulb. *Cell and Tissue Research*, *383*(1), 507–524. https://doi.org/10.1007/s00441-020-03365-9

Burton, S. D. (2017). Inhibitory circuits of the mammalian main olfactory bulb. *Journal of Neurophysiology*, *118*(4), 2034–2051. https://doi.org/10.1152/jn.00109.2017

Caillol, M., Aïoun, J., Baly, C., Persuy, M.-A., & Salesse, R. (2003). Localization of orexins and their receptors in the rat olfactory system: Possible modulation of olfactory perception by a neuropeptide synthetized centrally or locally. *Brain Research*, *960*(1), 48–61. https://doi.org/10.1016/S0006-8993(02)03755-1

Capsoni, S., Fogli Iseppe, A., Casciano, F., & Pignatelli, A. (2021). Unraveling the Role of Dopaminergic and Calretinin Interneurons in the Olfactory Bulb. *Frontiers in Neural Circuits*, *15*, 718221. https://doi.org/10.3389/fncir.2021.718221

Challet, E. (2019). The circadian regulation of food intake. *Nature Reviews Endocrinology*, *15*(7), 393–405. https://doi.org/10.1038/s41574-019-0210-x

Chen, K.-H. E., Lainez, N. M., Nair, M. G., & Coss, D. (2021). Visceral adipose tissue imparts peripheral macrophage influx into the hypothalamus. *Journal*

of Neuroinflammation, *18*(1), 140. https://doi.org/10.1186/s12974-021-02183-2

Cisternas, P., Salazar, P., Serrano, F. G., Montecinos-Oliva, C., Arredondo, S. B., Varela-Nallar, L., Barja, S., Vio, C. P., Gomez-Pinilla, F., & Inestrosa, N. C. (2015). Fructose consumption reduces hippocampal synaptic plasticity underlying cognitive performance. *Biochimica et Biophysica Acta (BBA) - Molecular Basis of Disease*, *1852*(11), 2379–2390. https://doi.org/10.1016/j.bbadis.2015.08.016

Coletti, A. M., Singh, D., Kumar, S., Shafin, T. N., Briody, P. J., Babbitt, B. F., Pan, D., Norton, E. S., Brown, E. C., Kahle, K. T., Del Bigio, M. R., & Conover, J. C. (2018). Characterization of the ventricular-subventricular stem cell niche during human brain development. *Development*, *145*(20), dev170100. https://doi.org/10.1242/dev.170100

Colín-Castelán, D., Ramírez-Santos, J., & Gutiérrez-Ospina, G. (2016). Differential vascular permeability along the forebrain ventricular neurogenic niche in the adult murine brain. *Journal of Neuroscience Research*, *94*(2), 161–169. https://doi.org/10.1002/jnr.23682

Colonna, M., & Butovsky, O. (2017). Microglia Function in the Central Nervous System During Health and Neurodegeneration. *Annual Review of Immunology*, *35*, 441–468. https://doi.org/10.1146/annurev-immunol-051116-052358

Cornell, J., Salinas, S., Huang, H.-Y., & Zhou, M. (2021). Microglia regulation of synaptic plasticity and learning and memory. *Neural Regeneration Research*, *17*(4), 705–716. https://doi.org/10.4103/1673-5374.322423

Cserép, C., Schwarcz, A. D., Pósfai, B., László, Z. I., Kellermayer, A., Környei, Z., Kisfali, M., Nyerges, M., Lele, Z., Katona, I., & Ádám Dénes. (2022). Microglial control of neuronal development via somatic purinergic junctions. *Cell Reports*, *40*(12), 111369. https://doi.org/10.1016/j.celrep.2022.111369

Daly, C. M., Saxena, J., Singh, J., Bullard, M. R., Bondy, E. O., Saxena, A., Buffalino, R. E., Melville, M. F., & Freeman, L. R. (2022). Sex Differences in Response to a High Fat, High Sucrose Diet in both the Gut Microbiome and Hypothalamic Astrocytes and Microglia. *Nutritional Neuroscience*, *25*(2), 321–335. https://doi.org/10.1080/1028415X.2020.1752996

De Marchis, S., Fasolo, A., & Puche, A. C. (2004). Subventricular zone-derived neuronal progenitors migrate into the subcortical forebrain of postnatal mice. *Journal of Comparative Neurology*, *476*(3), 290–300. https://doi.org/10.1002/cne.20217

de Oliveira Neves, V. G., de Oliveira, D. T., Oliveira, D. C., Oliveira Perucci, L., Dos Santos, T. A. P., da Costa Fernandes, I., de Sousa, G. G., Barboza, N. R., & Guerra-Sá, R. (2020). High-sugar diet intake, physical activity, and gut microbiota crosstalk: Implications for obesity in rats. *Food Science & Nutrition*, *8*(10), 5683–5695. https://doi.org/10.1002/fsn3.1842

De Souza, C. T., Araujo, E. P., Bordin, S., Ashimine, R., Zollner, R. L., Boschero, A. C., Saad, M. J. A., & Velloso, L. A. (2005). Consumption of a Fat-Rich Diet Activates a Proinflammatory Response and Induces Insulin Resistance in the Hypothalamus. *Endocrinology*, *146*(10), 4192–4199. https://doi.org/10.1210/en.2004-1520

Djordjevic, A., Bursać, B., Veličković, N., Vasiljević, A., & Matić, G. (2015). The impact of different fructose loads on insulin sensitivity, inflammation, and

PSA-NCAM-mediated plasticity in the hippocampus of fructose-fed male rats. *Nutritional Neuroscience*, *18*(2), 66–75. https://doi.org/10.1179/1476830513Y.0000000098

Dorfman, M. D., & Thaler, J. P. (2015). Hypothalamic inflammation and gliosis in obesity. *Current Opinion in Endocrinology, Diabetes and Obesity*, *22*(5), 325–330. https://doi.org/10.1097/MED.0000000000000182

Eriksson, P. S., Perfilieva, E., Björk-Eriksson, T., Alborn, A. M., Nordborg, C., Peterson, D. A., & Gage, F. H. (1998). Neurogenesis in the adult human hippocampus. *Nature Medicine*, *4*(11), 1313–1317. https://doi.org/10.1038/3305

Ernst, A., Alkass, K., Bernard, S., Salehpour, M., Perl, S., Tisdale, J., Possnert, G., Druid, H., & Frisén, J. (2014). Neurogenesis in the striatum of the adult human brain. *Cell*, *156*(5), 1072–1083. https://doi.org/10.1016/j.cell.2014.01.044

Escartin, C., Galea, E., Lakatos, A., O'Callaghan, J. P., Petzold, G. C., Serrano-Pozo, A., Steinhäuser, C., Volterra, A., Carmignoto, G., Agarwal, A., Allen, N. J., Araque, A., Barbeito, L., Barzilai, A., Bergles, D. E., Bonvento, G., Butt, A. M., Chen, W.-T., Cohen-Salmon, M., … Verkhratsky, A. (2021). Reactive astrocyte nomenclature, definitions, and future directions. *Nature Neuroscience*, *24*(3), 312–325. https://doi.org/10.1038/s41593-020-00783-4

Fernández Acosta, F. J., Luque-Molina, I., Vecino, R., Díaz-Guerra, E., Defterali, Ç., Pignatelli, J., & Vicario, C. (2022). Morphological Diversity of Calretinin Interneurons Generated From Adult Mouse Olfactory Bulb Core Neural Stem Cells. *Frontiers in Cell and Developmental Biology*, *10*. https://www.frontiersin.org/articles/10.3389/fcell.2022.932297

Fierros-Campuzano, J., Ballesteros-Zebadúa, P., Manjarrez-Marmolejo, J., Aguilera, P., Méndez-Diaz, M., Prospero-García, O., & Franco-Pérez, J. (2020). Irreversible hippocampal changes induced by high fructose diet in rats. *Nutritional Neuroscience*, *0*(0), 1–13. https://doi.org/10.1080/1028415X.2020.1853418

Fiorelli, R., Azim, K., Fischer, B., & Raineteau, O. (2015). Adding a spatial dimension to postnatal ventricular-subventricular zone neurogenesis. *Development*, *142*(12), 2109–2120. https://doi.org/10.1242/dev.119966

Fogli Iseppe, A., Pignatelli, A., & Belluzzi, O. (2016). Calretinin-Periglomerular Interneurons in Mice Olfactory Bulb: Cells of Few Words. *Frontiers in Cellular Neuroscience*, *10*, 231. https://doi.org/10.3389/fncel.2016.00231

Franco, I., Valdez-Tapia, M., Sanchez-Serrano, S. L., Cruz, S. L., & Lamas, M. (2014). Chronic toluene exposure induces cell proliferation in the mice SVZ but not migration through the RMS. *Neuroscience Letters*, *575*, 101–106. https://doi.org/10.1016/j.neulet.2014.05.043

Fujioka, T., Kaneko, N., & Sawamoto, K. (2019). Blood vessels as a scaffold for neuronal migration. *Neurochemistry International*, *126*, 69–73. https://doi.org/10.1016/j.neuint.2019.03.001

Gage, F. H. (2019). Adult neurogenesis in mammals. *Science (New York, N.Y.)*, *364*(6443), 827–828. https://doi.org/10.1126/science.aav6885

Gao, Y., Bielohuby, M., Fleming, T., Grabner, G. F., Foppen, E., Bernhard, W., Guzmán-Ruiz, M., Layritz, C., Legutko, B., Zinser, E., García-Cáceres, C., Buijs, R. M., Woods, S. C., Kalsbeek, A., Seeley, R. J., Nawroth, P. P., Bidlingmaier, M., Tschöp, M. H., & Yi, C.-X. (2017). Dietary sugars, not

lipids, drive hypothalamic inflammation. *Molecular Metabolism*, *6*(8), 897–908. https://doi.org/10.1016/j.molmet.2017.06.008

Gariepy, G., Nitka, D., & Schmitz, N. (2010). The association between obesity and anxiety disorders in the population: A systematic review and meta-analysis. *International Journal of Obesity*, *34*(3), 407–419. https://doi.org/10.1038/ijo.2009.252

Gaysinskaya, V. A., Karatayev, O., Shuluk, J., & Leibowitz, S. F. (2011). Hyperphagia induced by sucrose: Relation to circulating and CSF glucose and corticosterone and orexigenic peptides in the arcuate nucleus. *Pharmacology Biochemistry and Behavior*, *97*(3), 521–530. https://doi.org/10.1016/j.pbb.2010.10.008

GBD 2015 Obesity Collaborators, Afshin, A., Forouzanfar, M. H., Reitsma, M. B., Sur, P., Estep, K., Lee, A., Marczak, L., Mokdad, A. H., Moradi-Lakeh, M., Naghavi, M., Salama, J. S., Vos, T., Abate, K. H., Abbafati, C., Ahmed, M. B., Al-Aly, Z., Alkerwi, A., Al-Raddadi, R., … Murray, C. J. L. (2017). Health Effects of Overweight and Obesity in 195 Countries over 25 Years. *The New England Journal of Medicine*, *377*(1), 13–27. https://doi.org/10.1056/NEJMoa1614362

Getchell, T. V., Kwong, K., Saunders, C. P., Stromberg, A. J., & Getchell, M. L. (2006). Leptin regulates olfactory-mediated behavior in ob/ob mice. *Physiology & Behavior*, *87*(5), 848–856. https://doi.org/10.1016/j.physbeh.2005.11.016

Ginhoux, F., Greter, M., Leboeuf, M., Nandi, S., See, P., Gokhan, S., Mehler, M. F., Conway, S. J., Ng, L. G., Stanley, E. R., Samokhvalov, I. M., & Merad, M. (2010). Fate Mapping Analysis Reveals That Adult Microglia Derive from

Primitive Macrophages. *Science*, *330*(6005), 841–845. https://doi.org/10.1126/science.1194637

Götz, M., & Huttner, W. B. (2005). The cell biology of neurogenesis. *Nature Reviews Molecular Cell Biology*, *6*(10), 777–788. https://doi.org/10.1038/nrm1739

Graham, L. C., Harder, J. M., Soto, I., de Vries, W. N., John, S. W. M., & Howell, G. R. (2016). Chronic consumption of a western diet induces robust glial activation in aging mice and in a mouse model of Alzheimer's disease. *Scientific Reports*, *6*, 21568. https://doi.org/10.1038/srep21568

Guillamón-Vivancos, T., Gómez-Pinedo, U., & Matías-Guiu, J. (2015). Astrocytes in neurodegenerative diseases (I): Function and molecular description. *Neurología (English Edition)*, *30*(2), 119–129. https://doi.org/10.1016/j.nrleng.2014.12.005

Gunstad, J., Sanborn, V., & Hawkins, M. (2020). Cognitive dysfunction is a risk factor for overeating and obesity. *The American Psychologist*, *75*(2), 219–234. https://doi.org/10.1037/amp0000585

Guthoff, M., Tschritter, O., Berg, D., Liepelt, I., Schulte, C., Machicao, F., Haering, H.-U., & Fritsche, A. (2009). Effect of genetic variation in Kv1.3 on olfactory function. *Diabetes/Metabolism Research and Reviews*, *25*(6), 523–527. https://doi.org/10.1002/dmrr.979

Haynes, S. E., Hollopeter, G., Yang, G., Kurpius, D., Dailey, M. E., Gan, W.-B., & Julius, D. (2006). The P2Y12 receptor regulates microglial activation by extracellular nucleotides. *Nature Neuroscience*, *9*(12), 1512–1519. https://doi.org/10.1038/nn1805

Herzine, A., Laugeray, A., Feat, J., Menuet, A., Quesniaux, V., Richard, O., Pichon, J., Montécot-Dubourg, C., Perche, O., & Mortaud, S. (2016). Perinatal Exposure to Glufosinate Ammonium Herbicide Impairs Neurogenesis and Neuroblast Migration through Cytoskeleton Destabilization. *Frontiers in Cellular Neuroscience*, *10*, 191. https://doi.org/10.3389/fncel.2016.00191

Hill, J. M., Lesniak, M. A., Pert, C. B., & Roth, J. (1986). Autoradiographic localization of insulin receptors in rat brain: Prominence in olfactory and limbic areas. *Neuroscience*, *17*(4), 1127–1138. https://doi.org/10.1016/0306-4522(86)90082-5

Horvath, T. L., Sarman, B., García-Cáceres, C., Enriori, P. J., Sotonyi, P., Shanabrough, M., Borok, E., Argente, J., Chowen, J. A., Perez-Tilve, D., Pfluger, P. T., Brönneke, H. S., Levin, B. E., Diano, S., Cowley, M. A., & Tschöp, M. H. (2010). Synaptic input organization of the melanocortin system predicts diet-induced hypothalamic reactive gliosis and obesity. *Proceedings of the National Academy of Sciences*, *107*(33), 14875–14880. https://doi.org/10.1073/pnas.1004282107

Hsu, T. M., Konanur, V. R., Taing, L., Usui, R., Kayser, B. D., Goran, M. I., & Kanoski, S. E. (2015). Effects of sucrose and high fructose corn syrup consumption on spatial memory function and hippocampal neuroinflammation in adolescent rats. *Hippocampus*, *25*(2), 227–239. https://doi.org/10.1002/hipo.22368

Hua, J., Garcia de Paco, E., Linck, N., Maurice, T., Desrumaux, C., Manoury, B., Rassendren, F., & Ulmann, L. (2023). Microglial P2X4 receptors promote ApoE degradation and contribute to memory deficits in Alzheimer's disease.

Cellular and Molecular Life Sciences, *80*(5), 138. https://doi.org/10.1007/s00018-023-04784-x

Inta, D., Meyer-Lindenberg, A., & Gass, P. (2010). Alterations in Postnatal Neurogenesis and Dopamine Dysregulation in Schizophrenia: A Hypothesis. *Schizophrenia Bulletin*, *37*, 674–680. https://doi.org/10.1093/schbul/sbq134

Jacques, A., Chaaya, N., Beecher, K., Ali, S. A., Belmer, A., & Bartlett, S. (2019). The impact of sugar consumption on stress driven, emotional and addictive behaviors. *Neuroscience and Biobehavioral Reviews*, *103*, 178–199. https://doi.org/10.1016/j.neubiorev.2019.05.021

Jara, N., Cifuentes, M., Martínez, F., González-Chavarría, I., Salazar, K., Ferrada, L., & Nualart, F. (2022). Vitamin C Deficiency Reduces Neurogenesis and Proliferation in the SVZ and Lateral Ventricle Extensions of the Young Guinea Pig Brain. *Antioxidants*, *11*(10), 2030. https://doi.org/10.3390/antiox11102030

Jin, K., Sun, Y., Xie, L., Batteur, S., Mao, X. O., Smelick, C., Logvinova, A., & Greenberg, D. A. (2003). Neurogenesis and aging: FGF-2 and HB-EGF restore neurogenesis in hippocampus and subventricular zone of aged mice. *Aging Cell*, *2*(3), 175–183. https://doi.org/10.1046/j.1474-9728.2003.00046.x

Joers, V., Tansey, M. G., Mulas, G., & Carta, A. R. (2017). Microglial phenotypes in Parkinson's disease and animal models of the disease. *Progress in Neurobiology*, *155*, 57–75. https://doi.org/10.1016/j.pneurobio.2016.04.006

Johnsen, K. B., Burkhart, A., Melander, F., Kempen, P. J., Vejlebo, J. B., Siupka, P., Nielsen, M. S., Andresen, T. L., & Moos, T. (2017). Targeting transferrin receptors at the blood-brain barrier improves the uptake of immunoliposomes

and subsequent cargo transport into the brain parenchyma. *Scientific Reports*, *7*(1), 10396. https://doi.org/10.1038/s41598-017-11220-1

Kaneko, N., Marín, O., Koike, M., Hirota, Y., Uchiyama, Y., Wu, J. Y., Lu, Q., Tessier-Lavigne, M., Alvarez-Buylla, A., Okano, H., Rubenstein, J. L. R., & Sawamoto, K. (2010). New Neurons Clear the Path of Astrocytic Processes for Their Rapid Migration in the Adult Brain. *Neuron*, *67*(2), 213–223. https://doi.org/10.1016/j.neuron.2010.06.018

Kaushik, P., Gorin, F., & Vali, S. (2007). Dynamics of tyrosine hydroxylase mediated regulation of dopamine synthesis. *Journal of Computational Neuroscience*, *22*(2), 147–160. https://doi.org/10.1007/s10827-006-0004-8

Kelly, J. P., Wrynn, A. S., & Leonard, B. E. (1997). The olfactory bulbectomized rat as a model of depression: An update. *Pharmacology & Therapeutics*, *74*(3), 299–316. https://doi.org/10.1016/s0163-7258(97)00004-1

Kempermann, G., Gage, F. H., Aigner, L., Song, H., Curtis, M. A., Thuret, S., Kuhn, H. G., Jessberger, S., Frankland, P. W., Cameron, H. A., Gould, E., Hen, R., Abrous, D. N., Toni, N., Schinder, A. F., Zhao, X., Lucassen, P. J., & Frisén, J. (2018). Human Adult Neurogenesis: Evidence and Remaining Questions. *Cell Stem Cell*, *23*(1), 25–30. https://doi.org/10.1016/j.stem.2018.04.004

Kendig, M. D. (2014). Cognitive and behavioural effects of sugar consumption in rodents. A review. *Appetite*, *80*, 41–54. https://doi.org/10.1016/j.appet.2014.04.028

Kendig, M. D., Rooney, K. B., Corbit, L. H., & Boakes, R. A. (2014). Persisting adiposity following chronic consumption of 10% sucrose solution: Strain differences and behavioural effects. *Physiology & Behavior*, *130*, 54–65. https://doi.org/10.1016/j.physbeh.2014.03.021

Kettenmann, H., Kirchhoff, F., & Verkhratsky, A. (2013). Microglia: New Roles for the Synaptic Stripper. *Neuron*, *77*(1), 10–18. https://doi.org/10.1016/j.neuron.2012.12.023

Ketterer, C., Heni, M., Thamer, C., Herzberg-Schäfer, S. A., Häring, H.-U., & Fritsche, A. (2011). Acute, short-term hyperinsulinemia increases olfactory threshold in healthy subjects. *International Journal of Obesity*, *35*(8), 1135–1138. https://doi.org/10.1038/ijo.2010.251

Khakh, B. S., & Sofroniew, M. V. (2015). Diversity of astrocyte functions and phenotypes in neural circuits. *Nature Neuroscience*, *18*(7), 942–952. https://doi.org/10.1038/nn.4043

Kiyokage, E., Pan, Y.-Z., Shao, Z., Kobayashi, K., Szabo, G., Yanagawa, Y., Obata, K., Okano, H., Toida, K., Puche, A. C., & Shipley, M. T. (2010). Molecular Identity of Periglomerular and Short Axon Cells. *The Journal of Neuroscience*, *30*(3), 1185–1196. https://doi.org/10.1523/JNEUROSCI.3497-09.2010

Kohwi, M., Petryniak, M. A., Long, J. E., Ekker, M., Obata, K., Yanagawa, Y., Rubenstein, J. L. R., & Alvarez-Buylla, A. (2007). A Subpopulation of Olfactory Bulb GABAergic Interneurons Is Derived from Emx1- and Dlx5/6-Expressing Progenitors. *Journal of Neuroscience*, *27*(26), 6878–6891. https://doi.org/10.1523/JNEUROSCI.0254-07.2007

Konishi, M., Sakaguchi, M., Lockhart, S. M., Cai, W., Li, M. E., Homan, E. P., Rask-Madsen, C., & Kahn, C. R. (2017). Endothelial insulin receptors differentially control insulin signaling kinetics in peripheral tissues and brain of mice. *Proceedings of the National Academy of Sciences of the United*

States of America, *114*(40), E8478–E8487. https://doi.org/10.1073/pnas.1710625114

Kosaka, K., & Kosaka, T. (2007). Chemical properties of type 1 and type 2 periglomerular cells in the mouse olfactory bulb are different from those in the rat olfactory bulb. *Brain Research*, *1167*, 42–55. https://doi.org/10.1016/j.brainres.2007.04.087

Krout, K. E., Kawano, J., Mettenleiter, T. C., & Loewy, A. D. (2002). CNS inputs to the suprachiasmatic nucleus of the rat. *Neuroscience*, *110*(1), 73–92. https://doi.org/10.1016/s0306-4522(01)00551-6

Kubotera, H., Ikeshima-Kataoka, H., Hatashita, Y., Allegra Mascaro, A. L., Pavone, F. S., & Inoue, T. (2019). Astrocytic endfeet re-cover blood vessels after removal by laser ablation. *Scientific Reports*, *9*(1), 1263. https://doi.org/10.1038/s41598-018-37419-4

Lacar, B., Young, S. Z., Platel, J.-C., & Bordey, A. (2011). Gap junction-mediated calcium waves define communication networks among murine postnatal neural progenitor cells. *The European Journal of Neuroscience*, *34*(12), 1895–1905. https://doi.org/10.1111/j.1460-9568.2011.07901.x

Lainez, N. M., Jonak, C. R., Nair, M. G., Ethell, I. M., Wilson, E. H., Carson, M. J., & Coss, D. (2018). Diet-Induced Obesity Elicits Macrophage Infiltration and Reduction in Spine Density in the Hypothalami of Male but Not Female Mice. *Frontiers in Immunology*, *9*, 1992. https://doi.org/10.3389/fimmu.2018.01992

Lalli, G. (2014). Extracellular Signals Controlling Neuroblast Migration in the Postnatal Brain. In L. Nguyen & S. Hippenmeyer (Eds.), *Cellular and*

Molecular Control of Neuronal Migration (pp. 149–180). Springer Netherlands. https://doi.org/10.1007/978-94-007-7687-6_9

Lang, B. T., Yan, Y., Dempsey, R. J., & Vemuganti, R. (2009). Impaired neurogenesis in adult type-2 diabetic rats. *Brain Research, 1258,* 25–33. https://doi.org/10.1016/j.brainres.2008.12.026

Law, A. K. T., Pencea, V., Buck, C. R., & Luskin, M. B. (1999). Neurogenesis and Neuronal Migration in the Neonatal Rat Forebrain Anterior Subventricular Zone Do Not Require GFAP-Positive Astrocytes. *Developmental Biology*, *216*(2), 622–634. https://doi.org/10.1006/dbio.1999.9498

Lazarini, F., Mouthon, M.-A., Gheusi, G., Chaumont, F. de, Olivo-Marin, J.-C., Lamarque, S., Abrous, D. N., Boussin, F. D., & Lledo, P.-M. (2009). Cellular and Behavioral Effects of Cranial Irradiation of the Subventricular Zone in Adult Mice. *PLOS ONE*, *4*(9), e7017. https://doi.org/10.1371/journal.pone.0007017

Leiter, O., Zhuo, Z., Rust, R., Wasielewska, J. M., Grönnert, L., Kowal, S., Overall, R. W., Adusumilli, V. S., Blackmore, D. G., Southon, A., Ganio, K., McDevitt, C. A., Rund, N., Brici, D., Mudiyan, I. A., Sykes, A. M., Rünker, A. E., Zocher, S., Ayton, S., … Walker, T. L. (2022). Selenium mediates exercise-induced adult neurogenesis and reverses learning deficits induced by hippocampal injury and aging. *Cell Metabolism*, *34*(3), 408-423.e8. https://doi.org/10.1016/j.cmet.2022.01.005

Li, J., Wu, H., Liu, Y., & Yang, L. (2020). High fat diet induced obesity model using four strainsof mice: Kunming, C57BL/6, BALB/c and ICR. *Experimental Animals*, *69*(3), 326–335. https://doi.org/10.1538/expanim.19-0148

Li, J.-M., Ge, C.-X., Xu, M.-X., Wang, W., Yu, R., Fan, C.-Y., & Kong, L.-D. (2015). Betaine recovers hypothalamic neural injury by inhibiting astrogliosis and inflammation in fructose-fed rats. *Molecular Nutrition & Food Research*, *59*(2), 189–202. https://doi.org/10.1002/mnfr.201400307

Li, J.-M., Yu, R., Zhang, L.-P., Wen, S.-Y., Wang, S.-J., Zhang, X.-Y., Xu, Q., & Kong, L.-D. (2019). Dietary fructose-induced gut dysbiosis promotes mouse hippocampal neuroinflammation: A benefit of short-chain fatty acids. *Microbiome*, *7*(1), 98. https://doi.org/10.1186/s40168-019-0713-7

Lim, D. A., & Alvarez-Buylla, A. (2014). Adult neural stem cells stake their ground. *Trends in Neurosciences*, *37*(10), 563–571. https://doi.org/10.1016/j.tins.2014.08.006

Lim, D. A., & Alvarez-Buylla, A. (2016). The Adult Ventricular-Subventricular Zone (V-SVZ) and Olfactory Bulb (OB) Neurogenesis. *Cold Spring Harbor Perspectives in Biology*, *8*(5), a018820. https://doi.org/10.1101/cshperspect.a018820

Lin, T. K., Teymourian, Y., & Tursini, M. S. (2018). The effect of sugar and processed food imports on the prevalence of overweight and obesity in 172 countries. *Globalization and Health*, *14*(1), 35. https://doi.org/10.1186/s12992-018-0344-y

Loiola, R. A., García-Gabilondo, M., Grayston, A., Bugno, P., Kowalska, A., Duban-Deweer, S., Rizzi, E., Hachani, J., Sano, Y., Shimizu, F., Kanda, T., Mysiorek, C., Mazurek, M. P., Rosell, A., & Gosselet, F. (2021). Secretome of endothelial progenitor cells from stroke patients promotes endothelial barrier tightness and protects against hypoxia-induced vascular leakage. *Stem*

Cell Research & Therapy, *12*, 552. https://doi.org/10.1186/s13287-021-02608-y

Long, J. M., & Holtzman, D. M. (2019). Alzheimer Disease: An Update on Pathobiology and Treatment Strategies. *Cell*, *179*(2), 312–339. https://doi.org/10.1016/j.cell.2019.09.001

Loprinzi, P. D., & Frith, E. (2018). Obesity and episodic memory function. *The Journal of Physiological Sciences: JPS*, *68*(4), 321–331. https://doi.org/10.1007/s12576-018-0612-x

Luger, M., Lafontan, M., Bes-Rastrollo, M., Winzer, E., Yumuk, V., & Farpour-Lambert, N. (2017). Sugar-Sweetened Beverages and Weight Gain in Children and Adults: A Systematic Review from 2013 to 2015 and a Comparison with Previous Studies. *Obesity Facts*, *10*(6), 674–693. https://doi.org/10.1159/000484566

Luppino, F. S., de Wit, L. M., Bouvy, P. F., Stijnen, T., Cuijpers, P., Penninx, B. W. J. H., & Zitman, F. G. (2010). Overweight, Obesity, and Depression: A Systematic Review and Meta-analysis of Longitudinal Studies. *Archives of General Psychiatry*, *67*(3), 220–229. https://doi.org/10.1001/archgenpsychiatry.2010.2

Ma, Z., Stork, T., Bergles, D. E., & Freeman, M. R. (2016). Neuromodulators signal through astrocytes to alter neural circuit activity and behaviour. *Nature*, *539*(7629), 428–432. https://doi.org/10.1038/nature20145

Machado, P. P., Steele, E. M., Louzada, M. L. da C., Levy, R. B., Rangan, A., Woods, J., Gill, T., Scrinis, G., & Monteiro, C. A. (2020). Ultra-processed food consumption drives excessive free sugar intake among all age groups in

Australia. *European Journal of Nutrition*, *59*(6), 2783–2792. https://doi.org/10.1007/s00394-019-02125-y

Macrides, F., & Schneider, S. P. (1982). Laminar organization of mitral and tufted cells in the main olfactory bulb of the adult hamster. *The Journal of Comparative Neurology*, *208*(4), 419–430. https://doi.org/10.1002/cne.902080410

Malik, V. S., Pan, A., Willett, W. C., & Hu, F. B. (2013). Sugar-sweetened beverages and weight gain in children and adults: A systematic review and meta-analysis. *The American Journal of Clinical Nutrition*, *98*(4), 1084–1102. https://doi.org/10.3945/ajcn.113.058362

Martončíková, M., Alexovič Matiašová, A., Ševc, J., & Račeková, E. (2021). Relationship between Blood Vessels and Migration of Neuroblasts in the Olfactory Neurogenic Region of the Rodent Brain. *International Journal of Molecular Sciences*, *22*(21), 11506. https://doi.org/10.3390/ijms222111506

Martoncikova, M., Fabianova, K., Schreiberova, A., Blasko, J., Almasiova, V., & Racekova, E. (2014). Astrocytic and vascular scaffolding for neuroblast migration in the rostral migratory stream. *Current Neurovascular Research*, *11*(4), 321–329. https://doi.org/10.2174/1567202611666140903121253

Matsuno, T., Kiyokage, E., & Toida, K. (2017). Synaptic distribution of individually labeled mitral cells in the external plexiform layer of the mouse olfactory bulb. *Journal of Comparative Neurology*, *525*(7), 1633–1648. https://doi.org/10.1002/cne.24148

Meller, S. J., Hernandez, L., Martin-Lopez, E., Kloos, Z. A., Liberia, T., & Greer, C. A. (2023). Microglia Maintain Homeostatic Conditions in the Developing

Rostral Migratory Stream. *ENeuro*, *10*(2), ENEURO.0197-22.2023. https://doi.org/10.1523/ENEURO.0197-22.2023

Meo, S. A., Altuwaym, A. A., Alfallaj, R. M., Alduraibi, K. A., Alhamoudi, A. M., Alghamdi, S. M., & Akram, A. (2019). Effect of Obesity on Cognitive Function among School Adolescents: A Cross-Sectional Study. *Obesity Facts*, *12*(2), 150–156. https://doi.org/10.1159/000499386

Merkle, F. T., Fuentealba, L. C., Sanders, T. A., Magno, L., Kessaris, N., & Alvarez-Buylla, A. (2014). Adult neural stem cells in distinct microdomains generate previously unknown interneuron types. *Nature Neuroscience*, *17*(2), 207–214. https://doi.org/10.1038/nn.3610

Merkle, F. T., Mirzadeh, Z., & Alvarez-Buylla, A. (2007). Mosaic Organization of Neural Stem Cells in the Adult Brain. *Science*, *317*(5836), 381–384. https://doi.org/10.1126/science.1144914

Miller, A. A., & Spencer, S. J. (2014). Obesity and neuroinflammation: A pathway to cognitive impairment. *Brain, Behavior, and Immunity*, *42*, 10–21. https://doi.org/10.1016/j.bbi.2014.04.001

Mirzadeh, Z., Merkle, F. T., Soriano-Navarro, M., García-Verdugo, J. M., & Alvarez-Buylla, A. (2008). Neural stem cells confer unique pinwheel architecture to the ventricular surface in neurogenic regions of the adult brain. *Cell Stem Cell*, *3*(3), 265–278. https://doi.org/10.1016/j.stem.2008.07.004

Mizrak, D., Levitin, H. M., Delgado, A. C., Crotet, V., Yuan, J., Chaker, Z., Silva-Vargas, V., Sims, P. A., & Doetsch, F. (2019). Single-Cell Analysis of Regional Differences in Adult V-SVZ Neural Stem Cell Lineages. *Cell Reports*, *26*(2), 394-406.e5. https://doi.org/10.1016/j.celrep.2018.12.044

Moody, L. R., Barrett-Wilt, G. A., Sussman, M. R., & Messing, A. (2017). Glial fibrillary acidic protein exhibits altered turnover kinetics in a mouse model of alexander disease. *The Journal of Biological Chemistry*, *292*(14), 5814–5824. https://doi.org/10.1074/jbc.M116.772020

Mori, K., Manabe, H., Narikiyo, K., & Onisawa, N. (2013). Olfactory consciousness and gamma oscillation couplings across the olfactory bulb, olfactory cortex, and orbitofrontal cortex. *Frontiers in Psychology*, *4*, 743. https://doi.org/10.3389/fpsyg.2013.00743

Nagayama, S., Homma, R., & Imamura, F. (2014). Neuronal organization of olfactory bulb circuits. *Frontiers in Neural Circuits*, *8*, 98. https://doi.org/10.3389/fncir.2014.00098

Najac, M., Sanz Diez, A., Kumar, A., Benito, N., Charpak, S., & De Saint Jan, D. (2015). Intraglomerular Lateral Inhibition Promotes Spike Timing Variability in Principal Neurons of the Olfactory Bulb. *The Journal of Neuroscience*, *35*(10), 4319–4331. https://doi.org/10.1523/JNEUROSCI.2181-14.2015

Naritsuka, H., Sakai, K., Hashikawa, T., Mori, K., & Yamaguchi, M. (2009). Perisomatic-targeting granule cells in the mouse olfactory bulb. *The Journal of Comparative Neurology*, *515*(4), 409–426. https://doi.org/10.1002/cne.22063

Nicolis di Robilant, V., Scardigli, R., Strimpakos, G., Tirone, F., Middei, S., Scopa, C., De Bardi, M., Battistini, L., Saraulli, D., & Farioli Vecchioli, S. (2019). Running-Activated Neural Stem Cells Enhance Subventricular Neurogenesis and Improve Olfactory Behavior in p21 Knockout Mice. *Molecular Neurobiology*, *56*(11), 7534–7556. https://doi.org/10.1007/s12035-019-1590-6

Nishizumi, H., Miyashita, A., Inoue, N., Inokuchi, K., Aoki, M., & Sakano, H. (2019). Primary dendrites of mitral cells synapse unto neighboring glomeruli independent of their odorant receptor identity. *Communications Biology*, *2*, 14. https://doi.org/10.1038/s42003-018-0252-y

Noguchi, T., Utsugi, C., & Kashiwayanagi, M. (2017). Soft-diet feeding impairs neural transmission between mitral cells and interneurons in the mouse olfactory bulb. *Archives of Oral Biology*, *83*, 209–213. https://doi.org/10.1016/j.archoralbio.2017.07.015

Obernier, K., & Alvarez-Buylla, A. (2019). Neural stem cells: Origin, heterogeneity and regulation in the adult mammalian brain. *Development (Cambridge, England)*, *146*(4), dev156059. https://doi.org/10.1242/dev.156059

OECD. (2019, October 10). *The Heavy Burden of Obesity: The Economics of Prevention | en | OECD*. https://www.oecd.org/health/the-heavy-burden-of-obesity-67450d67-en.htm

Orona, E., Scott, J. W., & Rainer, E. C. (1983). Different granule cell populations innervate superficial and deep regions of the external plexiform layer in rat olfactory bulb. *The Journal of Comparative Neurology*, *217*(2), 227–237. https://doi.org/10.1002/cne.902170209

Ortega, F., Berninger, B., & Costa, M. R. (2013). Primary culture and live imaging of adult neural stem cells and their progeny. *Methods in Molecular Biology (Clifton, N.J.)*, *1052*, 1–11. https://doi.org/10.1007/7651_2013_22

Ortega, F., Gascón, S., Masserdotti, G., Deshpande, A., Simon, C., Fischer, J., Dimou, L., Chichung Lie, D., Schroeder, T., & Berninger, B. (2013). Oligodendrogliogenic and neurogenic adult subependymal zone neural stem cells constitute distinct lineages and exhibit differential responsiveness to

Wnt signalling. *Nature Cell Biology*, *15*(6), Article 6. https://doi.org/10.1038/ncb2736

Palouzier-Paulignan, B., Lacroix, M.-C., Aimé, P., Baly, C., Caillol, M., Congar, P., Julliard, A. K., Tucker, K., & Fadool, D. A. (2012). Olfaction under metabolic influences. *Chemical Senses*, *37*(9), 769–797. https://doi.org/10.1093/chemse/bjs059

Paredes, M. F., James, D., Gil-Perotin, S., Kim, H., Cotter, J. A., Ng, C., Sandoval, K., Rowitch, D. H., Xu, D., McQuillen, P. S., Garcia-Verdugo, J.-M., Huang, E. J., & Alvarez-Buylla, A. (2016). Extensive migration of young neurons into the infant human frontal lobe. *Science*, *354*(6308), aaf7073. https://doi.org/10.1126/science.aaf7073

Parrish-Aungst, S., Shipley, M. T., Erdelyi, F., Szabo, G., & Puche, A. C. (2007). Quantitative analysis of neuronal diversity in the mouse olfactory bulb. *The Journal of Comparative Neurology*, *501*(6), 825–836. https://doi.org/10.1002/cne.21205

Patkar, O. L., Belmer, A., Beecher, K., Jacques, A., & Bartlett, S. E. (2019). Pindolol Rescues Anxiety-Like Behavior and Neurogenic Maladaptations of Long-Term Binge Alcohol Intake in Mice. *Frontiers in Behavioral Neuroscience*, *13*. https://doi.org/10.3389/fnbeh.2019.00264

Peretto, P., Giachino, C., Aimar, P., Fasolo, A., & Bonfanti, L. (2005). Chain formation and glial tube assembly in the shift from neonatal to adult subventricular zone of the rodent forebrain. *The Journal of Comparative Neurology*, *487*(4), 407–427. https://doi.org/10.1002/cne.20576

Peretto, P., Merighi, A., Fasolo, A., & Bonfanti, L. (1999). The subependymal layer in rodents: A site of structural plasticity and cell migration in the adult

mammalian brain. *Brain Research Bulletin*, *49*(4), 221–243. https://doi.org/10.1016/s0361-9230(99)00037-4

Pinching, A. J., & Powell, T. P. (1971). The neuron types of the glomerular layer of the olfactory bulb. *Journal of Cell Science*, *9*(2), 305–345. https://doi.org/10.1242/jcs.9.2.305

Powley, T. L. (2000). Vagal circuitry mediating cephalic-phase responses to food. *Appetite*, *34*(2), 184–188. https://doi.org/10.1006/appe.1999.0279

PwC Australia. (2015). *Weighing the cost of obesity: A case for action*. https://www.pwc.com.au/pdf/weighing-the-cost-of-obesity-final.pdf

Quintana, F. J. (2017). Astrocytes to the rescue! Glia limitans astrocytic endfeet control CNS inflammation. *The Journal of Clinical Investigation*, *127*(8), 2897–2899. https://doi.org/10.1172/JCI95769

Rasool, D., Soleimani, V. D., & Jahani-Asl, A. (2022). Isolation of Adult Mouse Neural Stem Cells and Assessment of Self-Renewal by ELDA. In A. Jahani-Asl (Ed.), *Neuronal Cell Death: Methods and Protocols* (pp. 343–354). Springer US. https://doi.org/10.1007/978-1-0716-2409-8_21

Ribeiro Xavier, A. L., Kress, B. T., Goldman, S. A., Lacerda de Menezes, J. R., & Nedergaard, M. (2015). A Distinct Population of Microglia Supports Adult Neurogenesis in the Subventricular Zone. *The Journal of Neuroscience*, *35*(34), 11848–11861. https://doi.org/10.1523/JNEUROSCI.1217-15.2015

Rodríguez-Gómez, J. A., Kavanagh, E., Engskog-Vlachos, P., Engskog, M. K. R., Herrera, A. J., Espinosa-Oliva, A. M., Joseph, B., Hajji, N., Venero, J. L., & Burguillos, M. A. (2020). Microglia: Agents of the CNS Pro-Inflammatory Response. *Cells*, *9*(7), 1717. https://doi.org/10.3390/cells9071717

Sakamoto, M., Ieki, N., Miyoshi, G., Mochimaru, D., Miyachi, H., Imura, T., Yamaguchi, M., Fishell, G., Mori, K., Kageyama, R., & Imayoshi, I. (2014). Continuous Postnatal Neurogenesis Contributes to Formation of the Olfactory Bulb Neural Circuits and Flexible Olfactory Associative Learning. *The Journal of Neuroscience*, *34*(17), 5788–5799. https://doi.org/10.1523/JNEUROSCI.0674-14.2014

Salvadó, G., Milà-Alomà, M., Shekari, M., Ashton, N. J., Operto, G., Falcon, C., Cacciaglia, R., Minguillon, C., Fauria, K., Niñerola-Baizán, A., Perissinotti, A., Benedet, A. L., Kollmorgen, G., Suridjan, I., Wild, N., Molinuevo, J. L., Zetterberg, H., Blennow, K., Suárez-Calvet, M., … ALFA Study. (2022). Reactive astrogliosis is associated with higher cerebral glucose consumption in the early Alzheimer's continuum. *European Journal of Nuclear Medicine and Molecular Imaging*, *49*(13), 4567–4579. https://doi.org/10.1007/s00259-022-05897-4

Sanai, N., Nguyen, T., Ihrie, R. A., Mirzadeh, Z., Tsai, H.-H., Wong, M., Gupta, N., Berger, M. S., Huang, E., Garcia-Verdugo, J.-M., Rowitch, D. H., & Alvarez-Buylla, A. (2011). Corridors of migrating neurons in the human brain and their decline during infancy. *Nature*, *478*(7369), 382–386. https://doi.org/10.1038/nature10487

Schoenfeld, T. A., Marchand, J. E., & Macrides, F. (1985). Topographic organization of tufted cell axonal projections in the hamster main olfactory bulb: An intrabulbar associational system. *The Journal of Comparative Neurology*, *235*(4), 503–518. https://doi.org/10.1002/cne.902350408

Schoppa, N. E., & Urban, N. N. (2003). Dendritic processing within olfactory bulb circuits. *Trends in Neurosciences*, *26*(9), 501–506. https://doi.org/10.1016/S0166-2236(03)00228-5

Sellgren, C. M., Gracias, J., Watmuff, B., Biag, J. D., Thanos, J. M., Whittredge, P. B., Fu, T., Worringer, K., Brown, H. E., Wang, J., Kaykas, A., Karmacharya, R., Goold, C. P., Sheridan, S. D., & Perlis, R. H. (2019). Increased synapse elimination by microglia in schizophrenia patient-derived models of synaptic pruning. *Nature Neuroscience*, *22*(3), 374–385. https://doi.org/10.1038/s41593-018-0334-7

Serlin, Y., Shelef, I., Knyazer, B., & Friedman, A. (2015). Anatomy and Physiology of the Blood-Brain Barrier. *Seminars in Cell & Developmental Biology*, *38*, 2–6. https://doi.org/10.1016/j.semcdb.2015.01.002

Shah, P. T., Stratton, J. A., Stykel, M. G., Abbasi, S., Sharma, S., Mayr, K. A., Koblinger, K., Whelan, P. J., & Biernaskie, J. (2018). Single-Cell Transcriptomics and Fate Mapping of Ependymal Cells Reveals an Absence of Neural Stem Cell Function. *Cell*, *173*(4), 1045-1057.e9. https://doi.org/10.1016/j.cell.2018.03.063

Shao, Z., Puche, A. C., Kiyokage, E., Szabo, G., & Shipley, M. T. (2009). Two GABAergic Intraglomerular Circuits Differentially Regulate Tonic and Phasic Presynaptic Inhibition of Olfactory Nerve Terminals. *Journal of Neurophysiology*, *101*(4), 1988–2001. https://doi.org/10.1152/jn.91116.2008

Siddiqui, T. A., Lively, S., & Schlichter, L. C. (2016). Complex molecular and functional outcomes of single versus sequential cytokine stimulation of rat microglia. *Journal of Neuroinflammation*, *13*. https://doi.org/10.1186/s12974-016-0531-9

Snapyan, M., Lemasson, M., Brill, M. S., Blais, M., Massouh, M., Ninkovic, J., Gravel, C., Berthod, F., Götz, M., Barker, P. A., Parent, A., & Saghatelyan, A. (2009). Vasculature guides migrating neuronal precursors in the adult mammalian forebrain via brain-derived neurotrophic factor signaling. *Journal of Neuroscience*, *29*(13), 4172–4188. Scopus. https://doi.org/10.1523/JNEUROSCI.4956-08.2009

Sofroniew, M. V. (2009). Molecular dissection of reactive astrogliosis and glial scar formation. *Trends in Neurosciences*, *32*(12), 638–647. https://doi.org/10.1016/j.tins.2009.08.002

Sorrells, S. F., Paredes, M. F., Cebrian-Silla, A., Sandoval, K., Qi, D., Kelley, K. W., James, D., Mayer, S., Chang, J., Auguste, K. I., Chang, E. F., Gutierrez, A. J., Kriegstein, A. R., Mathern, G. W., Oldham, M. C., Huang, E. J., Garcia-Verdugo, J. M., Yang, Z., & Alvarez-Buylla, A. (2018). Human hippocampal neurogenesis drops sharply in children to undetectable levels in adults. *Nature*, *555*(7696), 377–381. https://doi.org/10.1038/nature25975

Sorrells, S. F., Paredes, M. F., Zhang, Z., Kang, G., Pastor-Alonso, O., Biagiotti, S., Page, C. E., Sandoval, K., Knox, A., Connolly, A., Huang, E. J., Garcia-Verdugo, J. M., Oldham, M. C., Yang, Z., & Alvarez-Buylla, A. (2021). Positive Controls in Adults and Children Support That Very Few, If Any, New Neurons Are Born in the Adult Human Hippocampus. *The Journal of Neuroscience: The Official Journal of the Society for Neuroscience*, *41*(12), 2554–2565. https://doi.org/10.1523/JNEUROSCI.0676-20.2020

Stogsdill, J. A., Ramirez, J., Liu, D., Kim, Y.-H., Baldwin, K. T., Enustun, E., Ejikeme, T., Ji, R.-R., & Eroglu, C. (2017). Astrocytic Neuroligins Control

Astrocyte Morphogenesis and Synaptogenesis. *Nature*, *551*(7679), 192. https://doi.org/10.1038/nature24638

Suyama, S., Sunabori, T., Kanki, H., Sawamoto, K., Gachet, C., Koizumi, S., & Okano, H. (2012). Purinergic signaling promotes proliferation of adult mouse subventricular zone cells. *The Journal of Neuroscience: The Official Journal of the Society for Neuroscience*, *32*(27), 9238–9247. https://doi.org/10.1523/JNEUROSCI.4001-11.2012

Takahashi, H., Yoshihara, S., & Tsuboi, A. (2018). The Functional Role of Olfactory Bulb Granule Cell Subtypes Derived From Embryonic and Postnatal Neurogenesis. *Frontiers in Molecular Neuroscience*, *11*, 229. https://doi.org/10.3389/fnmol.2018.00229

Tam, W. Y., & Ma, C. H. E. (2014). Bipolar/rod-shaped microglia are proliferating microglia with distinct M1/M2 phenotypes. *Scientific Reports*, *4*, 7279. https://doi.org/10.1038/srep07279

Tang, Y., & Le, W. (2016). Differential Roles of M1 and M2 Microglia in Neurodegenerative Diseases. *Molecular Neurobiology*, *53*(2), 1181–1194. https://doi.org/10.1007/s12035-014-9070-5

Tavazoie, M., Van der Veken, L., Silva-Vargas, V., Louissaint, M., Colonna, L., Zaidi, B., Garcia-Verdugo, J. M., & Doetsch, F. (2008). A specialized vascular niche for adult neural stem cells. *Cell Stem Cell*, *3*(3), 279–288. https://doi.org/10.1016/j.stem.2008.07.025

Thaler, J. P., & Schwartz, M. W. (2010). Minireview: Inflammation and Obesity Pathogenesis: The Hypothalamus Heats Up. *Endocrinology*, *151*(9), 4109–4115. https://doi.org/10.1210/en.2010-0336

Tong, J., Mannea, E., Aimé, P., Pfluger, P. T., Yi, C.-X., Castaneda, T. R., Davis, H. W., Ren, X., Pixley, S., Benoit, S., Julliard, K., Woods, S. C., Horvath, T. L., Sleeman, M. M., D'Alessio, D., Obici, S., Frank, R., & Tschöp, M. H. (2011). Ghrelin Enhances Olfactory Sensitivity and Exploratory Sniffing in Rodents and Humans. *The Journal of Neuroscience*, *31*(15), 5841–5846. https://doi.org/10.1523/JNEUROSCI.5680-10.2011

Torres-Platas, S. G., Nagy, C., Wakid, M., Turecki, G., & Mechawar, N. (2016). Glial fibrillary acidic protein is differentially expressed across cortical and subcortical regions in healthy brains and downregulated in the thalamus and caudate nucleus of depressed suicides. *Molecular Psychiatry*, *21*(4), Article 4. https://doi.org/10.1038/mp.2015.65

Tremblay, M.-E., Stevens, B., Sierra, A., Wake, H., Bessis, A., & Nimmerjahn, A. (2011). The Role of Microglia in the Healthy Brain. *Journal of Neuroscience*, *31*(45), 16064–16069. https://doi.org/10.1523/JNEUROSCI.4158-11.2011

Tufo, C., Poopalasundaram, S., Dorrego-Rivas, A., Ford, M. C., Graham, A., & Grubb, M. S. (2022). Development of the mammalian main olfactory bulb. *Development (Cambridge, England)*, *149*(3), dev200210. https://doi.org/10.1242/dev.200210

Urbán, N., & Guillemot, F. (2014). Neurogenesis in the embryonic and adult brain: Same regulators, different roles. *Frontiers in Cellular Neuroscience*, *8*, 396. https://doi.org/10.3389/fncel.2014.00396

Utsugi, C., Miyazono, S., Osada, K., Sasajima, H., Noguchi, T., Matsuda, M., & Kashiwayanagi, M. (2014). Hard-Diet Feeding Recovers Neurogenesis in the Subventricular Zone and Olfactory Functions of Mice Impaired by Soft-Diet Feeding. *PLoS ONE*, *9*(5). https://doi.org/10.1371/journal.pone.0097309

Valdearcos, M., Douglass, J. D., Robblee, M. M., Dorfman, M. D., Stifler, D. R., Bennett, M. L., Gerritse, I., Fasnacht, R., Barres, B. A., Thaler, J. P., & Koliwad, S. K. (2017). Microglial Inflammatory Signaling Orchestrates the Hypothalamic Immune Response to Dietary Excess and Mediates Obesity Susceptibility. *Cell Metabolism*, *26*(1), 185-197.e3. https://doi.org/10.1016/j.cmet.2017.05.015

van der Borght, K., Köhnke, R., Göransson, N., Deierborg, T., Brundin, P., Erlanson-Albertsson, C., & Lindqvist, A. (2011). Reduced neurogenesis in the rat hippocampus following high fructose consumption. *Regulatory Peptides*, *167*(1), 26–30. https://doi.org/10.1016/j.regpep.2010.11.002

Wang, C., Liu, F., Liu, Y.-Y., Zhao, C.-H., You, Y., Wang, L., Zhang, J., Wei, B., Ma, T., Zhang, Q., Zhang, Y., Chen, R., Song, H., & Yang, Z. (2011). Identification and characterization of neuroblasts in the subventricular zone and rostral migratory stream of the adult human brain. *Cell Research*, *21*(11), Article 11. https://doi.org/10.1038/cr.2011.83

Whitman, M. C., Fan, W., Rela, L., Rodriguez-Gil, D. J., & Greer, C. A. (2009). Blood vessels form a migratory scaffold in the rostral migratory stream. *The Journal of Comparative Neurology*, *516*(2), 94–104. https://doi.org/10.1002/cne.22093

Wu, A., Yu, B., Chen, Q., Matthews, G. A., Lu, C., Campbell, E., Tye, K. M., & Komiyama, T. (2020). Context-dependent plasticity of adult-born neurons regulated by cortical feedback. *Science Advances*, *6*(42), eabc8319. https://doi.org/10.1126/sciadv.abc8319

Wu, N., Chen, Y., Yang, J., & Li, F. (2017). Childhood Obesity and Academic Performance: The Role of Working Memory. *Frontiers in Psychology*, *8*, 611. https://doi.org/10.3389/fpsyg.2017.00611

Wu, Y.-K., & Berry, D. C. (2018). Impact of weight stigma on physiological and psychological health outcomes for overweight and obese adults: A systematic review. *Journal of Advanced Nursing*, *74*(5), 1030–1042. https://doi.org/10.1111/jan.13511

Yadirgi, G., & Marino, S. (2009). Adult neural stem cells and their role in brain pathology. *The Journal of Pathology*, *217*(2), 242–253. https://doi.org/10.1002/path.2480

Zhang, R. L., Chopp, M., Roberts, C., Liu, X., Wei, M., Nejad-Davarani, S. P., Wang, X., & Zhang, Z. G. (2014). Stroke Increases Neural Stem Cells and Angiogenesis in the Neurogenic Niche of the Adult Mouse. *PLOS ONE*, *9*(12), e113972. https://doi.org/10.1371/journal.pone.0113972

Zhang, X., Dong, H., Zhang, S., Lu, S., Sun, J., & Qian, Y. (2015). Enhancement of LPS-induced microglial inflammation response via TLR4 under high glucose conditions. *Cellular Physiology and Biochemistry: International Journal of Experimental Cellular Physiology, Biochemistry, and Pharmacology*, *35*(4), 1571–1581. https://doi.org/10.1159/000373972

Zhou, B., Zuo, Y.-X., & Jiang, R.-T. (2019). Astrocyte morphology: Diversity, plasticity, and role in neurological diseases. *CNS Neuroscience & Therapeutics*, *25*(6), 665–673. https://doi.org/10.1111/cns.13123